



UNIVERSITAT POLITÈCNICA
DE CATALUNYA
BARCELONATECH



MASTER THESIS

Development of the automation and control of a microgravity experiment by means of LabVIEW.

Alejandro Dias Pierres

SUPERVISED BY

Dr Ricard González Cinca

Universitat Politècnica de Catalunya
Master in Aerospace Science & Technology
- of 2022

This Page Intentionally Left Blank

Development of the automation and control of a microgravity experiment by means of LabVIEW.

BY

Alejandro Dias Pierres

DIPLOMA THESIS FOR MASTER

Master in Aerospace Science and Technology

AT

Universitat Politècnica de Catalunya

SUPERVISED BY:

Director's name: Ricard González Cinca

Department of the director: Space Exploration Lab

This Page Intentionally Left Blank

ABSTRACT

This master's thesis is part of an experimental project carried out at the Space Exploration Laboratory of the Universitat Politècnica de Catalunya, by a five master's students team, under the guidance of Ricard Gonzalez Cinca, to study the use of acoustic waves, for heat transfer enhancement, in a gas medium and with the innovation of been done under microgravity conditions, which have never been done before.

The objective of the experiment is to obtain new knowledge in this field, which might help Scientifics develop a new version of a thermal control system. The students had the opportunity to experiment under microgravity conditions, by being selected for the Drop Your Thesis Programme, provided by ESA academy, allowing the students to develop the experiment at the Space Exploration Laboratory and test it in the ZARM drop tower.

The experiment was divided into different subsystems: mechanical, software, electronics, mathematical simulations and testing. Each subsystem was developed by one of the master's students. This master thesis is focused on the software part of the experiment, designed using LabVIEW from National Instruments.

This document is divided into three main parts, starting with the introduction to the experiment, which explains the experiment background information, as well as the "Your Thesis Programme", then it continues with the introduction of the experiment software platform, LabVIEW. The thesis finalises with an explanation of the experiment control software developed.

This Page Intentionally Left Blank

Table of Contents

CHAPTER 1 INTRODUCTION	1
1.1. Experiment Background information.	3
1.2. Previous experiments in gas-phase medium.	4
1.3. Experiment objectives.....	5
1.4. Your thesis Programme	5
CHAPTER 2 EXPERIMENT SET UP	8
2.1. Heat Generator	9
2.2. Acoustic wave generator	10
2.3. Thermocouples	11
2.4. High-Speed camera	11
2.5. LEDs Matrix	12
2.6. Matrix MXC-4000 series.....	12
2.7. MyRIO-1900.	14
CHAPTER 3 CONTROL SOFTWARE	15
3.1. Basis of the software.....	15
3.1.1. LabVIEW Data Acquisition Basic Blocks	15
3.1.2. MyRIO main blocks.....	17
3.1.3. Matrix MXC-4000 main blocks.....	19
3.1.4. SubVIs Functionalities	20
3.2. Control Software for Laboratory experiments.....	22
3.2.1. Experiment Flow Diagram	23
3.2.2. MyRIO-1900 VI	25
3.2.3. Matrix MXC-4000 VI	32
3.3. Control software for Drop Tower Experiments.....	35
3.3.1. Experimental Procedure	35
3.3.2. MyRIO-1900 VI	36
3.3.3. Matrix MXC-4000 VI	38
CHAPTER 4 CONCLUSION	40
CHAPTER 5 BIBLIOGRAPHY	41
5.1. Articles:.....	41
5.2. Web Pages.....	42
5.3. Datasheets:.....	42
5.4. Thesis.....	42

This Page Intentionally Left Blank

List of Figures

- Figure 1.1 Loop Heat Pipe (LHP) Scheme [2]..... 2
- Figure 2.1: Experiment Set Up and Zoom inside Test cell 8
- Figure 2.2: Power vs Frequency for PZT 1 and PZT2.....11
- Figure 2.3 Matric MXC-4000 series12
- Figure 2.4: LabVIEW Project VI13
- Figure 2.5 MyRIO-190014
- Figure 3.1 Shared Variable.....16
- Figure 3.2 Open/Create/Replace file block16
- Figure 3.3 Write Delimited Spreadsheet17
- Figure 3.4 Open and Close MyRIO block diagrams.....18
- Figure 3.5 Read and Write block diagrams.....19
- Figure 3.6 Matrix MXC-4000, Initialize and Close block diagram19
- Figure 3.7 Matrix MXC-4000, configuration block diagram20
- Figure 3.8 Analog Input Express VI21
- Figure 3.9 Analog input Express VI code.....21
- Figure 3.10 Digital Output Express VI.....22
- Figure 3.11 Digital Output Express VI code22
- Figure 3.12 Experiment Flow Diagram24
- Figure 3.13 Thermocouples code25
- Figure 3.14 MyRIO pins in use26
- Figure 3.15 Data acquisition initialization [18].....27
- Figure 3.16 Data acquisition and housekeeping [18]28
- Figure 3.17 Accelerometer code.....29
- Figure 3.18 Heater trigger and LED trigger.....29
- Figure 3.19 Time Trigger30
- Figure 3.20 Experiment timer30
- Figure 3.21 Triggers Paths31
- Figure 3.22 MyRIO-1900 Control Panel.....32
- Figure 3.23 PZT code [18].....33
- Figure 3.24 Matrix MXC-4000 control panel34
- Figure 3.25 Updated Thermocouples code.....36
- Figure 3.26 Updated Heater Trigger code37
- Figure 3.27 Updated MyRIO-1900 VI control panel38
- Figure 3.28 Updated PZT code39
- Figure 3.29 Updated Matrix MXC-4000 VI control panel.....39

This Page Intentionally Left Blank

List of tables

Table 2.1: Heater Trade-off Analysis 9

Table 3.1 Experimental Procedure35

This Page Intentionally Left Blank

Chapter 1

INTRODUCTION

Currently, interest in the aerospace industry is increasing exponentially, meaning that further research is developed daily to satisfy the need for new and more challenging space exploration missions.

As weight is an essential factor in the space industry, smaller and more powerful devices have been developed. Meaning that the temperature that these devices can achieve is also increasing. This is an important issue mainly in electronics, as each electronic device has a specific operating temperature range, which often differs from one device to another.

Keeping the electronic components in the operating temperature range is a must. Otherwise, the components will malfunction, which results in the use of thermal control systems. There are two main categories: active and passive control systems. The difference between active and passive control systems is the use of an external power source. Passive control systems do not need an external power source, whereas active control systems need an external power supply.

Apart from the power consumption, the absence of gravity makes the design of new thermal control systems a more significant challenge. On Earth, gravity creates buoyancy-induced convection, which makes the heat generated by any device rise to the atmosphere. In contrast to on Earth, in microgravity, this effect does not occur, due to the absence of buoyancy, making the heat generated by the device stay around it, creating a bubble of heat.

At this point, the cooling devices used in microgravity are based on single-phase thermal control devices. As the heat generated by the components increases, the two-phase thermal control devices take the interest of scientists. However, the two-phase systems have problems to be solved before it overtakes the position of being the primary thermal control system in space applications.

The reason behind using the two-phase thermal control systems is the greater efficiency of two-phase systems compared to single-phase systems in terms of cooling.

An example of a two-phase thermal control device is the loop heat pipe (LHP) [1]. As shown in figure 1.1, where fluid in its liquid state flows through a porous evaporator covered by a metallic casing, where the heat flux occurs. The fluid, now in the vapour state, enters a condenser to change again to its liquid state and repeat the cycle.

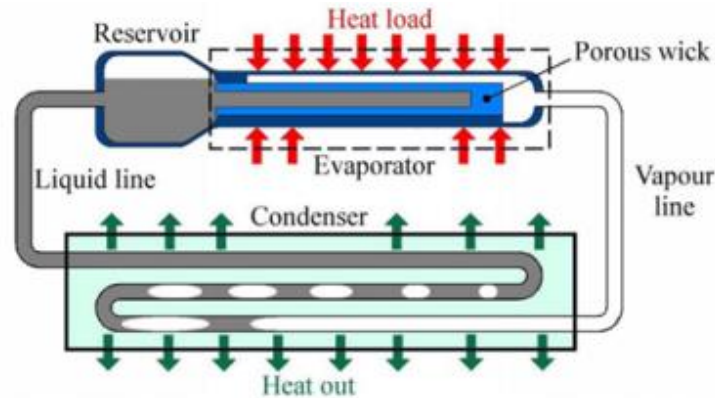


Figure 1.1 Loop Heat Pipe (LHP) Scheme [2]

As mentioned before, the two-phase cooling device has a problem in microgravity. Due to the absence of buoyancy, vapour does not flow as it does on Earth. In the wall that is heated, bubbles are created. This is a problem as the main characteristic for the system to work is fluid flow. Therefore, having the bubbles attached to the wall is a significant problem.

However, a possible solution was revealed by the authors of the "Phase change cooling of spacecraft electronics: Terrestrial Reference Experiments Prior to ISS Microgravity Experiments" research paper [2]. The proposed solution was subcooling. This method would produce condensation on the top part of the bubbles, which would stop the bubbles from expanding. Other methods would be to design the heating surface with an asymmetrical sawtooth profile or using pressure difference to increase the vapour mobility.

This master's thesis experiment was funded by the Space Exploration Lab at the Universitat Politècnica de Catalunya. As a continuation of another experiment done in the Space Exploration Lab [3]. The previous experiment [3] studied acoustic actuation for cryogenic propellant management and storage. The results showed more than an 8% increase in heat flux on Earth and under microgravity conditions. The results of this experiment [3] initiated an interest in using acoustic waves as a heat transfer enhancement mechanism. The present experiment is centred on how acoustic waves can enhance air convection to increase the dissipated heat from an electronic device. The use of acoustic waves could also be an alternative solution to the problem mentioned in [1] related to using a Loop Heat Pipe (LHP) in microgravity, using the acoustic waves to move the bubbles attached to the pipes.

The experiment comprises several devices, a heater and a piezoelectric transducer (PZT) as the main experiment's components. The thermocouples and a high-speed camera make the data acquisition. A MyRIO-1900 is used to gather the data from the thermocouples and give signals to activate the heater and the PZT. Finally, the Matrix MXC-4000 is used to control the frequency and amplitude of the acoustic wave created by the PZT.

This master's thesis is mainly based on the software part of the experiment, explaining the function of the different devices used and the reason behind it. The experiment was developed and tested at the Space Exploration Laboratory and performed in the ZARM drop tower. Therefore, some aspects will differ from the laboratory and ZARM software design. All the software design was developed using LabVIEW.

This thesis is divided into five chapters, starting with an introduction to the experiment and previous experiments, as well as describing "your thesis programmes" and others programs that could provide the experiment with the possibility of testing the experiment under microgravity conditions.

Then, chapter 2 explains the experiment setup, describing all the components of the experiment while emphasizing the heat generator and the acoustic wave generator for being the experiment's main components and the MyRIO-1900 and Matrix MXC-4000 series for been the main components when developing the control software.

The control software is explained in chapter 3. It is divided into three sections, the basics of the software, the control software for the laboratory experiments and the control software for the drop tower experiments.

Chapters 4 and 5 consist of the conclusion of this master's thesis, summarising all the information delivered and the bibliography.

1.1. Experiment Background information.

The experiment developed to be used in microgravity is a thermal control system which increases transfer by using acoustics. Using acoustic waves is an exciting method to detach the bubbles from the heated surface mentioned in the LHP. However, it has also proven to be effective in terms of heat transfer enhancement.

Some studies have been researched before starting with the development of this experiment, such as the review done by Alessandro Franco [4], which mentions some parameters that highly affect convective heat transfer. Some of these parameters are the fluid's temperature, pressure, heater dimensions, and others. Apart from this, the characteristics of the wave are the most fundamental parameters to take into account.

Nevertheless, Alessandro Franco's review [4] also mentioned that the increase in heat transfer could get to values of 1000% in the best of conditions. The best heat transfer occurs when using a fluid in the liquid state in a subcooled condition. Nevertheless, this is only the best of the conditions, and relevant results have been obtained with fluids in the gas state. The heat transfer enhancement is optimized the slower the gas particles move. In addition, no mathematical model has been possible to be developed as the results varied a lot, even for experiments under similar conditions.

When using a piezoelectric transducer (PZT) to create an increase in convection, there are different methods to be considered. The method chosen for this experiment is known as an acoustically excited system. The acoustically excited system [4] method is defined as having an acoustic field applied in the fluid. Another method that was investigated was the mechanically excited system [4]. In this case, vibrations are

created directly on the surface of the heater. However, this method was rejected as the vibrations could influence the thermocouple's readings when placed close to the heater plate.

1.2. Previous experiments in gas-phase medium.

The field of acoustics is a very extended topic. In order to reduce its field, the research done was primarily focused on the use of acoustics waves in a gas-phase medium.

An acoustic wave is classified mainly based on its frequency and power. In terms of frequency, an acoustic wave can be categorized as sound waves, which are the ones inside of the human hearing range, and ultrasounds, ultrasounds are the waves that exceed the human hearing range.

Ultrasound waves are divided into two main groups, depending on the power and frequency of the wave. One group is known as power ultrasounds (>10 Watts) or low-frequency ultrasound (20 to 100kHz). The other group is known as low-power ultrasounds (<10 Watts) or very high-frequency ultrasound (>1MHz). [5]

Power ultrasounds can influence the medium that it is travelling. The way ultrasound influences the medium could create some phenomena. For example, acoustic cavitation, acoustic streaming, dissipation of the acoustic field, or a modification of the thermal boundary layer. [5]

Conversely, low-power ultrasounds act in a "very high frequency" that does not affect the medium. In addition, it is used for medical diagnosis or non-destructive material control. [5]

In general, an acoustic wave has a sinusoidal movement, but when a certain intensity is reached, the flow of the fluid changes from a sinusoidal flow to a vortex-like flow. This phenomenon is known as acoustic streaming [6]. The creation of acoustic streaming is related to the attenuation of the acoustic wave and the friction between the fluid and the vibrating object, the acoustic device. [7]

In our experiment, the use of thermocouples is almost mandatory, as it will provide us with mathematical data to then determine the heat transfer enhancement by using the Nusselt number, which is defined as:

$$Nu = hLk \quad (1.1)$$

In a research done by L. Slimani [9], a PZT is used to be the source of the acoustic wave. The experiment is based on a wind tunnel, where a heat source is present. The frequency used is 40kHz, the airspeed is 0.4 meters per second, and the PZT is placed in front of the heater. In this research, the Nusselt number was used again to determine the heat transfer enhancement, achieving a rise of 37.5% for this setup.

There was more research based on heat transfer enhancement using acoustics, as revealed by Talebi [10], which used a cylindrical tank with air as the medium. The cylinder contained an ultrasonic wave generator at the top and the heat source at the

bottom. In this case, the achieved heat transfer enhancement was 175%. As mentioned before, the heat transfer enhancement varies with the distance between the heat source and the acoustic device. By doubling the amplitude, an increase of 88% was reached in the heat transfer coefficient. In contrast, when the amplitude was equal to half of the distance between the two primary devices, the heat transfer enhancement was 83%.

In all the researches mentioned, the heat transfers between a heat source and a gas-state fluid can be enhanced by using acoustic fields. However, all the experiments were done under normal gravity, showing interest in studying this phenomenon occurring in microgravity.

1.3. Experiment objectives

This master's thesis experiment was developed to better understand the use of acoustic waves for heat transfer enhancement as a continuation of an experiment previously developed at the Space Exploration Lab [3]. This experiment's innovation is using acoustic waves in a gas medium under microgravity conditions for heat transfer enhancement. Something that no research found had done before.

1.4. Your thesis Programme

The possibility of using the ZARM drop tower was thanks to being selected for the drop your thesis programme, a programme provided by the European Space Agency. The Your thesis programme consists of 4 different "your thesis" programs, drop your thesis, spin your thesis, fly your thesis and Orbit your thesis. Each one of these programs has its advantages and disadvantages. In this chapter, basic information about each program will be provided. To explain the reasons behind applying to drop your thesis programme instead of any other programme.

Leaving the drop your thesis to be the last one, the first programme that will be explained is the fly your thesis programme (FYT) [11]. The most significant advantage of fly your thesis is the time the experiment is in microgravity. The programme is operated in Novespace in Bordeaux, France. The participants will have three flights with 31 parabolas per flight. Each parabola contains approximately 22 seconds of microgravity. Therefore, the experiment would be in microgravity for around 10 minutes per flight. This fact is, without a doubt, an advantage, as more data could be gathered in these 30 minutes. The problem here is the microgravity level that is achieved in each parabola. As the microgravity is done in an aircraft, the microgravity level is not 100% stable. This is because a human pilot controls the aircraft. Therefore, depending on the experiment, it could have a bad side to the data gathered. The estimated microgravity level is 10-2 on average.

The spin your thesis [11], as its name indicates, is a programme that spins the experiment, so instead of applying microgravity to the experiment, it would apply hypergravity. This could be interesting to see how the acoustic wave interacts with the

heater in hypergravity, but at least it is not the point of this experiment yet. Furthermore, the gravity affecting the experiment is not on one axis. However, the experiment would be affected by the earth's gravity and the induced acceleration done by spinning the experiment on a different axis. Therefore, this programme was the first one to be rejected.

Orbit your thesis [11] is a programme where students can send an experiment to the international space station (ISS). Out of all the "your thesis programme", it has the best conditions for the experiment, as the data gathering in microgravity is approximately four months, and the microgravity level is 10^{-6} . However, the programme is only available for teams with a PhD student. Therefore, it was impossible to consider it, as none of the students in this experiment were PhD students at that time. Alternatively, the "Orbit your thesis" should be considered if further research is done.

The chosen programme, drop your thesis programme (DYT) [11], has the best characteristics for a first approach on the subject. The programme is done in Bremen, Germany, at the ZARM drop tower. The drop tower has three different configurations, the drop, the catapult and the newly developed Gravitower.

The drop configuration is the oldest of the three, which started in the early 90s. In this case, the experiment is integrated inside a capsule which is then dropped from 120. The drop tower is the best of the three programmes, without counting "orbit your thesis", because where the capsule is launched or dropped, there is almost no air resistance, as the 120 meters' tube is in a near vacuum environment, which allows the experiment to experience a microgravity level of 10^{-6} . The disadvantage concerning the fly your thesis programme is the time the capsule is in microgravity, which in the case of the drop configuration is approximately 4,7 seconds. But the 4,7 seconds in microgravity can be increased to approximately 9.3 seconds with the second configuration.

The second configuration is the catapult, where the experiment is integrated into a similar capsule, but instead of being dropped, it is launched from the bottom of the tube. The microgravity level is the same, although the time of the catapult configuration varies, depending on the height that the capsule reaches. In addition, the catapult is firstly put under an average of 18g with a peak of 30g. However, in both cases, the deceleration of the capsule is of an average of 25g to a peak of 50g, which means that if the experiment was developed to withstand 50g, the 30g experienced when using the catapult should not be an issue.

Furthermore, the catapult, as well as the drop configuration, are repeated five times, so the total amount of time is 4.7 seconds times five drops or 9.3 seconds times five launches, giving a total of 23.5 seconds, in the case of the drop configuration and approximately 46.5 seconds, in the case of the catapult configuration.

The last and newest drop tower configuration is the Gravitower. The Gravitower is an active system which does not need the experiment to rest from drop to drop, which enables the experiment to perform numerous cycles. Gathering a higher amount of data, as 4 hours in the Gravitower are given in exchange for a drop tower drop/launch, the Gravitower also can control the microgravity level from 10^{-6} g to 1g. The Gravitower may sound like the best option for any experiment. However, the time of each cycle in

the Gravitower is approximately 2 seconds, which was a concise amount of time for this experiment.

Outside of the “your thesis” programme, other programs could be interesting for further research of heat transfer enhancement due to the use of acoustics. Such as the REXUS programme [12]. This programme, stabilized in 1995 by the SSC ESRANGE, invites student experiments to be launched in a sounding rocket (GPS-Orion-Rocket). The REXUS programme provides the experiment with approximately 3 minutes of microgravity time. The rocket reaches an altitude between 78 to 93km.

Using the REXUS programme or the Orbit your thesis programme could be the next step in studying this phenomenon, as the data collected would have been significantly increased.

Chapter 2

Experiment Set Up

In the introduction of this master's thesis, it is mentioned that the experiment developed is a continuation of a previous experiment [3], also designed and built at the Space Exploration Lab.

Figure 2.1 is an image taken from the final set-up at ZARM. The set-up consists of the experiment test cell and three parts: The heat generator, the acoustic wave generator and the data acquisition.

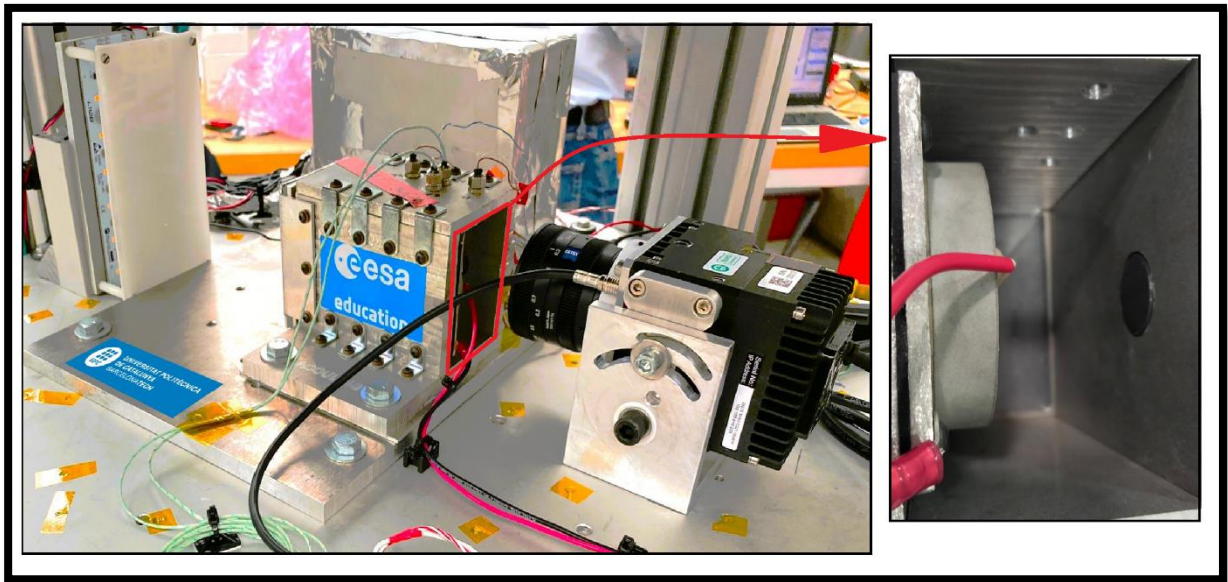


Figure 2.1: Experiment Set Up and Zoom inside Test cell

The heat generator consists of a heater plate that can create a uniform temperature field. The uniform temperature field is one of the most important criteria to keep in mind when choosing the heat source of the experiment.

The acoustic wave generator consists of a ceramic piezoelectric transducer and a function generator. The piezoelectric transducer and the heater plate are placed inside the test cell, one facing the other at a distance of 30 millimetres, see figure 2.1. The distance was determined using the Knudsen number. The Knudsen number is used to place the heat source at a high-density (and pressure) zone. This high-density (and pressure) zone is a node of the acoustic wave created by the PZT. The function generator (Matrix MXC-4000) is used to specify the frequency and amplitude of the acoustic wave created by the piezoelectric transducer.

The data acquisition consists of four thermocouples placed in front of the heater in a “4” form plus a thermocouple inside the heater. The right image of figure 2.1 shows four holes where the thermocouples are placed. The thermocouples are used to measure the heat transfer created by the propagation of the acoustic wave. In addition to the thermocouples, high-speed camera recordings are used to visualise density changes. The changes in density can be seen by applying Background Oriented Schlieren technique (BOS). In order to apply the BOS technique, the test cell must have two windows, one parallel to the other. One window must be transparent for the recording, and the other must contain a background pattern. The LED matrix is placed behind the patterned window to provide light for the recording. While the high-speed camera is provided and controlled by ZARM, the thermocouples are provided by the Space Exploration Lab and controlled by MyRIO. Furthermore, the data gathered from the thermocouples is saved in the internal memory of the MyRIO.

2.1. Heat Generator

The heat generator is one of the two main components of this master’s thesis experiment. The master’s student had the following options to choose a heat generator: Heating plate with heat flux sensor, Nichrome serpentine-shaped wire, Nichrome straight-shaped wire, Nichrome coil-shaped wire, Nichrome serpentine and aluminium plate and BACH RC ceramic resistor. The different options were put under test to create a trade-off Analysis table. The criteria are the following:

- Heat distribution – Generated heat flux allows easy analysis.
- Reliability – Level of security, redundancy and possibility of failure.
- Power consumption – Power required to reach the temperature needed.
- Structure and installation – Difficulty of installation/manufacturing
- Cost – Price of the overall heating system.
- Flexibility – Easiness to change the placement of the heater.

Table 2.1 contain all the results obtained from laboratory testing or provided by the datasheet. Each of the options for the heat generator were given a number from 1 to 6, which can be seen next to the “W” (which is a weight factor). The following list shows the number corresponding to the heat generator option.

1. Heating plate with heat flux sensor.
2. Nichrome serpentine shaped wire.
3. Nichrome straight shaped wire.
4. Nichrome coil shaped wire.
5. Nichrome serpentine and aluminium plate.
6. BACH RC ceramic resistor

Table 2.1: Heater Trade-off Analysis

Trade-off Analysis						
Criteria						

Solutions	W	1	2	3	4	5	6
<i>Heat distribution</i>	5	1	3	1	3	5	5
<i>Reliability</i>	5	1	4	4	4	3	5
<i>Power consumption</i>	3	5	4	1	4	3	4
<i>Structure and installation</i>	5	5	3	3	3	3	5
<i>Cost</i>	4	3	5	5	5	4	2
<i>Flexibility</i>	3	2	3	5	3	1	4
Score		68	91	78	91	83	107

As is shown in table 2.1, the type of heat generator used was the ceramic heating plate from BACH RC, with a circular and flat surface. The heater plate has a resistance of 9 ohms and can be powered to a maximum voltage of 24V, which means that the maximum power is 64W. The maximum temperature that the heater plate can withstand is 500°C. The temperature generated should be around 200°C at 1g to produce a heat flux that is strong enough to be seen in the BOS images. In addition, the BACH RC ceramic heating plate allows placing a thermocouple inside it.

2.2. Acoustic wave generator

In the case of the acoustic wave generator, three options were provided by the Space Exploration Lab. The first was a piezoelectric transducer (PZT) with a diameter of 50 mm and a thickness of 10 mm. The second option was also a piezoelectric transducer but with a 40 mm diameter and the same thickness, while the last option was a Langevin transducer.

Some research and simulations were done to determine which of the three options is the best. These simulations suggested that the pressure difference should be around 70 Pa to start seeing the effects of acoustic waves on heat transfer in a gas medium. The maximum pressure difference that the piezoelectric transducer could create was at the resonance frequency. The resonance frequency can be found by its relation with power consumption. The power consumption is higher at the resonance frequency of the piezoelectric transducer.

The power consumption was measured for the three options at different frequencies, from 5kHz to 65kHz. The following diagrams shown in figure 2.2 represent the test of both piezoelectric transducers as the Langevin was discarded for having a resonance frequency outside of this range.

Figure 2.2 shows the diagram of power against frequency for the two different piezoelectric transducers. The diagram on the left corresponds to the piezoelectric transducer with a diameter of 50 mm, while the one on the left corresponds to the PZT with a diameter of 40 mm.

As seen from the diagram of figure 2.2, the PZT with a diameter of 50 mm has a resonance frequency of 45 kHz. On the other hand, the PZT with a diameter of 40 mm has a resonance frequency of 54 kHz. Making the PZT with a diameter of 50 mm a better choice as a lower frequency produces a simpler acoustic field distribution. In addition, the wavelength will be bigger, making it easier when analysing the nodes and antinodes. This is also the reason when discarding the Langevin for having a higher resonance frequency than 65 kHz.

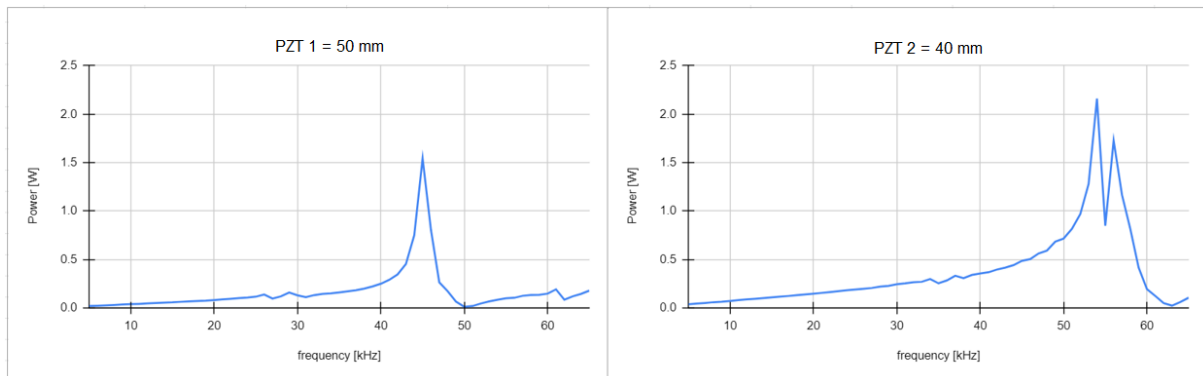


Figure 2.2: Power vs Frequency for PZT 1 and PZT 2

2.3. Thermocouples

The Space Exploration Lab provided the team with T-type thermocouples. The thermocouples were used to obtain numerical measurements, which would determine the heat transfer enhancement using the Nusselt number, as was done in other research papers [8].

The T-type thermocouples' operational temperature range is from 0°C to 250°C. As the temperature generated by the heater will reach a maximum of 200°C, the T-type thermocouples cover the experiment's needs. The data acquired from the T-type thermocouples goes through a circuit to filter the noise and is saved in the MyRIO-1900 internal memory, as mentioned at the end of this chapter's introduction.

2.4. High-Speed camera

The high-speed camera is the only camera in the experiment and is used for recording the phenomena occurring inside the test cell. It has been mentioned in the introduction of this experiment that the technique used to see the phenomena is the Background Oriented Schlieren (BOS).

During the development of the experiment, the high-speed camera used changed, using the Optronis camera provided by the Space Exploration Lab for the experiments done at the lab and the Photron FASTCAM MC2 provided by ZARM for the experiment

done at ZARM. Some tests were done at ZARM to know the distance between the test cell, the high-speed camera and the LEDs matrix to have a good resolution and focus on the experiment.

2.5. LEDs Matrix

The LEDs matrix PCB was designed and manufactured to provide the experiment with good lighting for the Background Oriented Schlieren technique. The LED matrix PCB is equipped with 21 LEDs to provide this good lighting. Seven rows containing three LEDs in each row.

2.6. Matrix MXC-4000 series

The Matrix MXC-4000 series, also known as function generator, is the central computer of the experiment. It is fanless and has a cable-less design, which makes it dependable in harsh environments, with resistance to severe temperature changes and vibrations. The Matrix MXC-4000 is an expandable embedded computer. Therefore, it can install a hot-pluggable fan module to dissipate heat generated within the system. Figure 2.3 shows a picture of the Matrix MXC-4000 series. [14]



Figure 2.3 Matric MXC-4000 series

The Matrix MXC-4000 has many different ports. The main ones used for the experiment and the ground tests are the following:

- Power Supply: DC Input (9-32 V)
- Capsule connection: GbE
- MyRIO connection: USB 2.0

Apart from the mentioned ports, two different modules were installed on the Matrix MXC-4000. The first module installed is the TE5325, which enables the Matrix MXC-4000 to act as a function generator. The second module installed is the TE3322, which is an amplifier. The test in microgravity used a different amplifier, but the TE3322 modules were used for the ground test.

For the use of the Matrix MXC-4000, two more ports were needed to control the computer. Therefore, a screen was attached to the VGA port and a mouse to one of the 4 USB 2.0 ports.

The Matrix MXC-4000 has three actions to carry out in this experiment. The first is the storage of the LabVIEW Project, which contains the LabVIEW codes (also known as VI) for the Matrix MXC-4000 and the MyRIO-1900, the VI that has to be executed by the Matrix MXC-4000 and the VI that has to be executed by the MyRIO-1900.

The second action is the communication between the Matrix MXC-4000 and the MyRIO-1900, which is done by interconnecting the MyRIO-1900 to the Matrix MXC-4000 using the USB device cable provided by the MyRIO.

The final action is done automatically by using the project VI instead of a standard VI to write the code, as in the project VI, it can be specified where the code has to be executed. This is shown in figure 2.4. The blue rectangles represent the Matrix MXC-4000 and the code for this computer, while the red rectangles represent the MyRIO-1900 and the code that the MyRIO will execute.

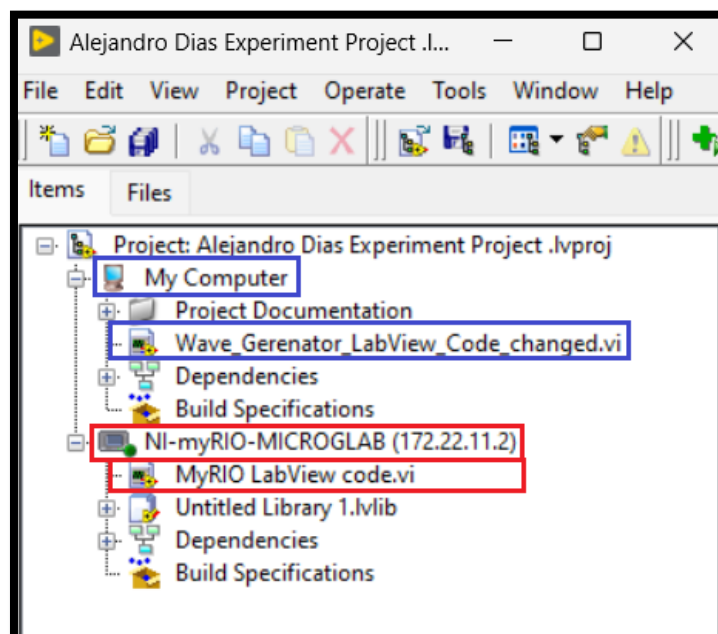


Figure 2.4: LabVIEW Project VI

2.7. MyRIO-1900.

The MyRIO-1900, shown in figure 2.5, is a portable reconfigurable I/O device used in the experiment as a data acquisition system (DAS). Other devices could be used instead of the MyRIO-1900. However, the MyRIO-1900 is a product developed by National instruments, as well as the company that developed the software used for this experiment, LabVIEW. MyRIO has the best compatibility with the chosen software, easing the learning process. [13]



Figure 2.5 MyRIO-1900

The MyRIO-1900 provides different ports that were used in the experiment:

- Power supply port (cable)
- USB Device cable
- Connector Pinouts (A and B)
- Connector C

The USB Device cable is the one that connects the MyRIO-1900 to the Matrix MXC-4000. Connector Pinouts A and B contain four Analog inputs for data gathering, which measure voltages between 0 and 5 volts. It also contains an Analog ground and sixteen digital inputs/outputs, with an output of 3.3 voltages and a compatible input of 3.3/5 voltages. The connector also contains a digital ground and a five voltages power supply output. The ports from connector C that were used are the five-voltage power supply, the digital ground and the two high-impedance, differential Analog input channels, which have a range between -10 voltages and +10 voltages.

Chapter 3

Control Software

This chapter is based on the development of the control software design. The code was constantly changed due to needing a clearer idea of the experiment process from the beginning. Therefore, this chapter shows two similar but different codes. One for the experiments at the Space Exploration Lab and another for the Drop Tower experiments.

3.1. Basis of the software.

LabVIEW is a software development platform which National Instruments created and, for the past 35 years, has been the tool chosen by engineers to develop automated test systems for the design of software that can measure, test, validate and research in real-time. The meaning behind its name is “Laboratory Virtual Instrumentation Engineering Workbench”. [15]

In the drop tower, everything is controlled using LabVIEW VIs designed by the ZARM engineers. In addition, the drop tower capsule contains hardware designed by National Instrument, such as the PXI.

The NI PXI system provides high-performance modular instrumentation, apart from other modules that consist of specialized synchronization and other modules that are key in the software for testing applications. [16]

Summarizing, using LabVIEW was the best choice in terms of developing the software for the experiment, as the Space Exploration Lab provided the team with a MyRIO-1900, a Matrix MXC-4000, as well as the necessary libraries. Further, the drop tower capsule used a NI PXI, which, as well as LabVIEW and MyRIO-1900, are part of National Instruments. Therefore, using LabVIEW, which was already available using the university license, was the best possible choice for software development.

3.1.1. LabVIEW Data Acquisition Basic Blocks

In this subchapter, some blocks will be described to simplify the description of the Data Acquisition block of the LabVIEW Software Design. The main block to be described are the shared variable, the Open/create/replace file and the Write Delimited Spreadsheet.

3.1.1.1. Share Variables

The shared variable is a simple block with the functionality to share input from one VI to another inside the same project. This block will be seen mainly in the data acquisition, as the data acquisition code is written in the MyRIO VI, whereas the data from the PZT, like the frequency output and the amplitude, is coded in the Matrix MXC-4000 VI. Figure 3.1 shows the shared variable block. The block's colour will change depending on the kind of value it is sharing, Boolean, numeric, string, etc.



Figure 3.1 Shared Variable

3.1.1.2. Open/Create/Replace file

The primary function of this block is, as its name indicates, it is the ability to interact with a file. By using a control, the user can choose between opening an existing file, creating a new one, or replacing the content of an existing file with new content. Before so, a file path must be introduced so that when the code runs, LabVIEW knows where to create the file. In the case of choosing the replace function, apart from the folder where you want the file to be created, the file to be replaced must also be stated. Otherwise, an error will be delivered.

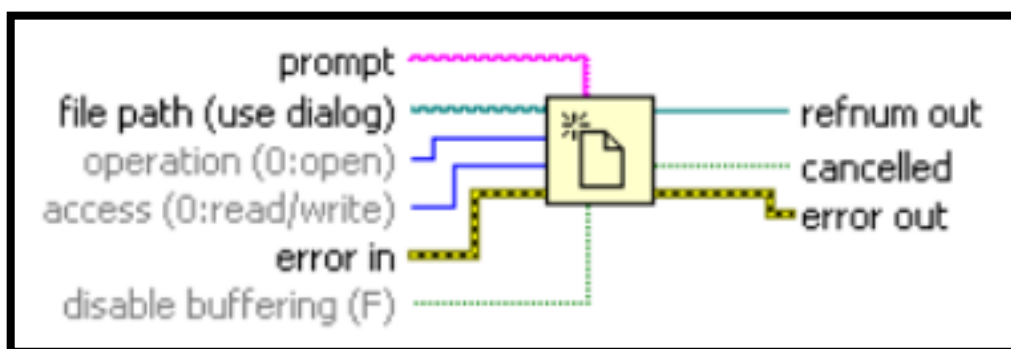


Figure 3.2 Open/Create/Replace file block

3.1.1.3. Write Delimited Spreadsheet

The Write Delimited Spreadsheet VI, shown in figure 3.3, is used to convert a 2D or 1D array of strings, signed integers, or double-precision numbers to a text string. It also writes the data provided to it, to a new or existing file. The file to which it will write the data is determined in the file path input, whereas in the case of the data acquisition, it uses the block described in the previous section, 3.1.1.2 Open/Create/Replace file.

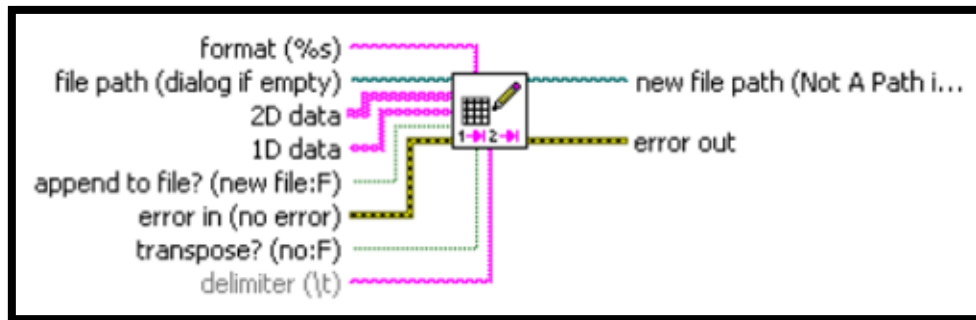


Figure 3.3 Write Delimited Spreadsheet

3.1.2. MyRIO main blocks.

This section will describe the different MyRIO blocks used in the software design, this blocks were mainly used for the activation of physical triggers and the data acquisition of the thermocouples.

The blocks are divided in two different kinds, the “open and close” blocks and the “write and read”.

3.1.2.1. Open and Close block diagrams.

The MyRIO uses three different types of open blocks, as shown in figure 3.4. The first one is the Smart Open used by the Analog Input and Digital Output Express VI. This block can open an I/O reference the first time it runs and then save the reference in the memory. It ensures the Express VI runs efficiently in loops.

In contrast, the Open block opens an I/O reference channel for each interaction, which makes it less efficient. Maximum and minimum values can be stated for the Open block, but it was not necessary for this experiment software.

The MyRIO DIO Open block functions as the Open block just mentioned, but it is used for the digital input and output, whereas the Open block works for the Analog input and output.

Finally, all the Open blocks, except for the Smart open, need to use a close block to close the references for data operation.

Figure 3.4 shows the diagrams of the four types of blocks mentioned above.

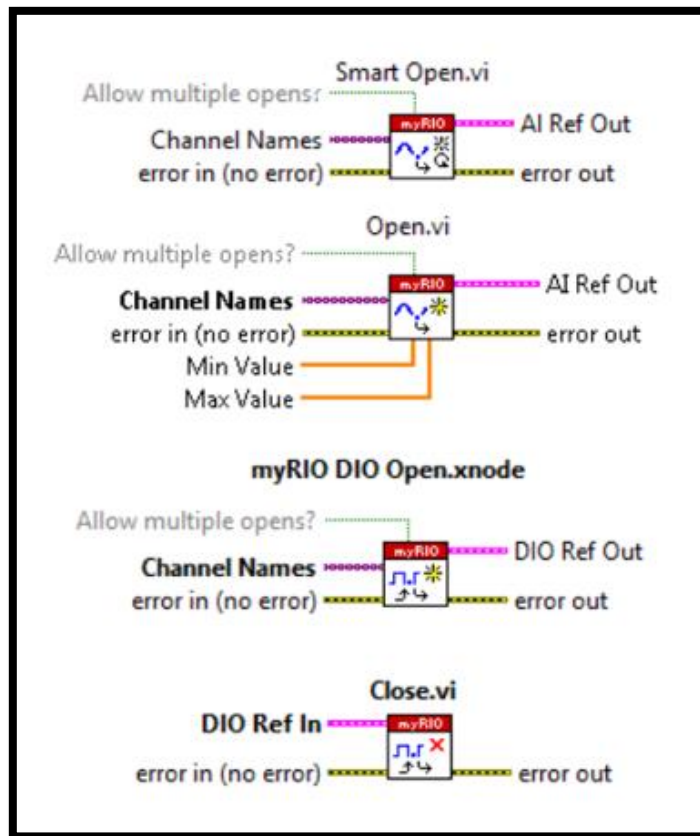


Figure 3.4 Open and Close MyRIO block diagrams

3.1.2.2. Read and Write block diagrams

In figure 3.5, two different blocks are shown, the first block is the Read block diagram which is used to show the values obtained from an Analog or digital input. The other block is the write block diagram which is used in the experiment to send a 3.3V signal through the digital I/O, which is used as a trigger.

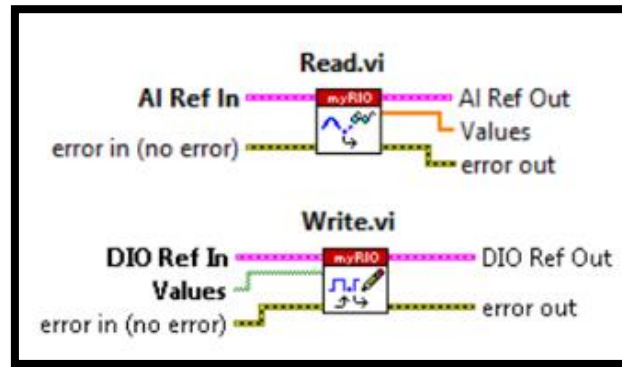


Figure 3.5 Read and Write block diagrams

3.1.3. Matrix MXC-4000 main blocks

The Matrix MXC-4000 has its own blocks in LabVIEW, which do not come with LabVIEW by default, meaning that some drivers have to be installed in order to operate with this device. [18]

The Matrix MXC-4000 utilize similar blocks as the MyRIO-1900, the blocks used in the experiment are divided in to families, the initialize and close block diagrams and the configurations blocks.

3.1.3.1. Initialize and Close block diagrams

The initialize block shown in figure 3.6, open a new session, to the specified device in the resource name, depending in the structure and who the code was designed, it will send initialization commands to the rest of the blocks, as for the close block, it is the last one in the chain, used to finalize the session in the Matrix MXC-4000.

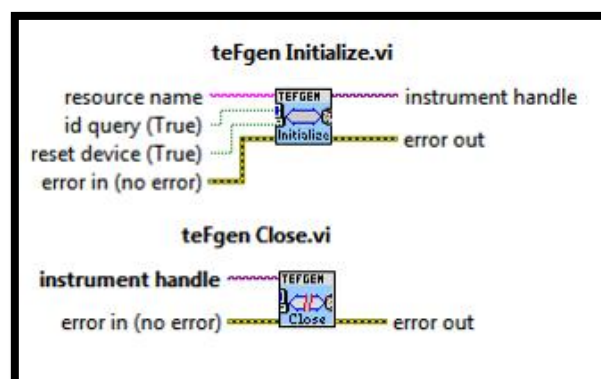


Figure 3.6 Matrix MXC-4000, Initialize and Close block diagram

3.1.3.2. Configuration block diagrams

The configuration blocks, shown in figure 3.7 are used for: Obtain the model number, specify the frequency of the PZT, the amplitude and when the acoustic wave should be turned one.

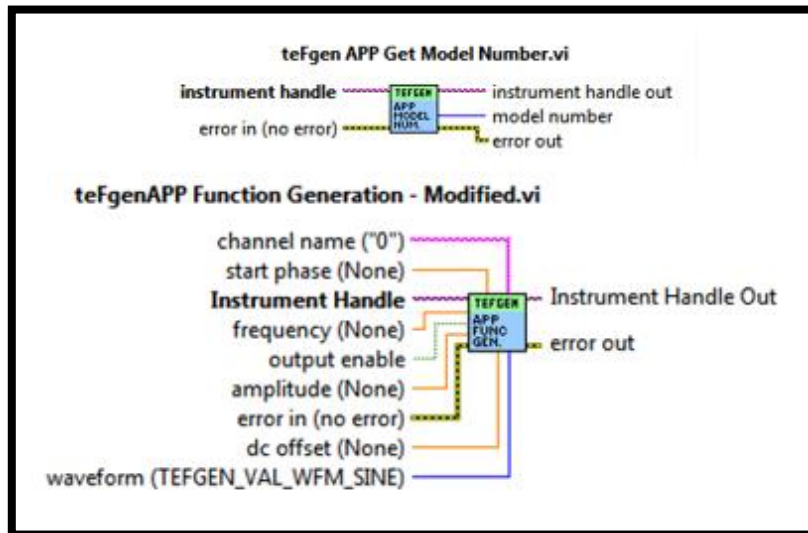


Figure 3.7 Matrix MXC-4000, configuration block diagram

3.1.4. SubVIs Functionalities

Apart from blocks, which have a simple functionality, there are block which can be opened and observe a new VI, this blocks are known as SubVIs. The SubVIs that will be described here are the Analog Input Express VI and the Digital Output Express VI, which correspond to the thermocouples code and the heater trigger/5V signal code.

3.1.4.1. Analog Input Express VI

Figure 3.8, shows the Analog input Express VI, which uses the blocks mentioned in sections 3.1.2.1 and 3.1.2.2, to read the data from Connectors A, B or C. The Analog input Express VI code is shows in figure 3.9.

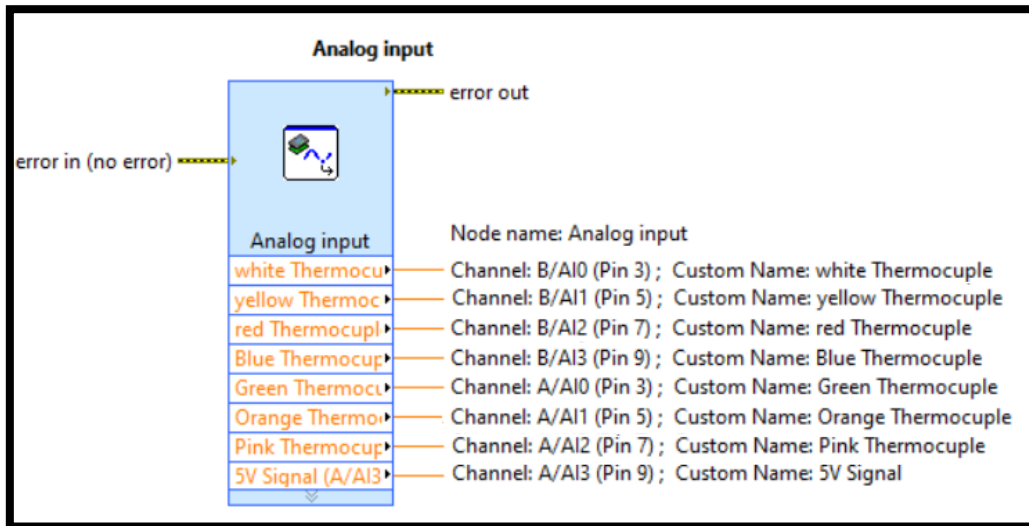


Figure 3.8 Analog Input Express VI

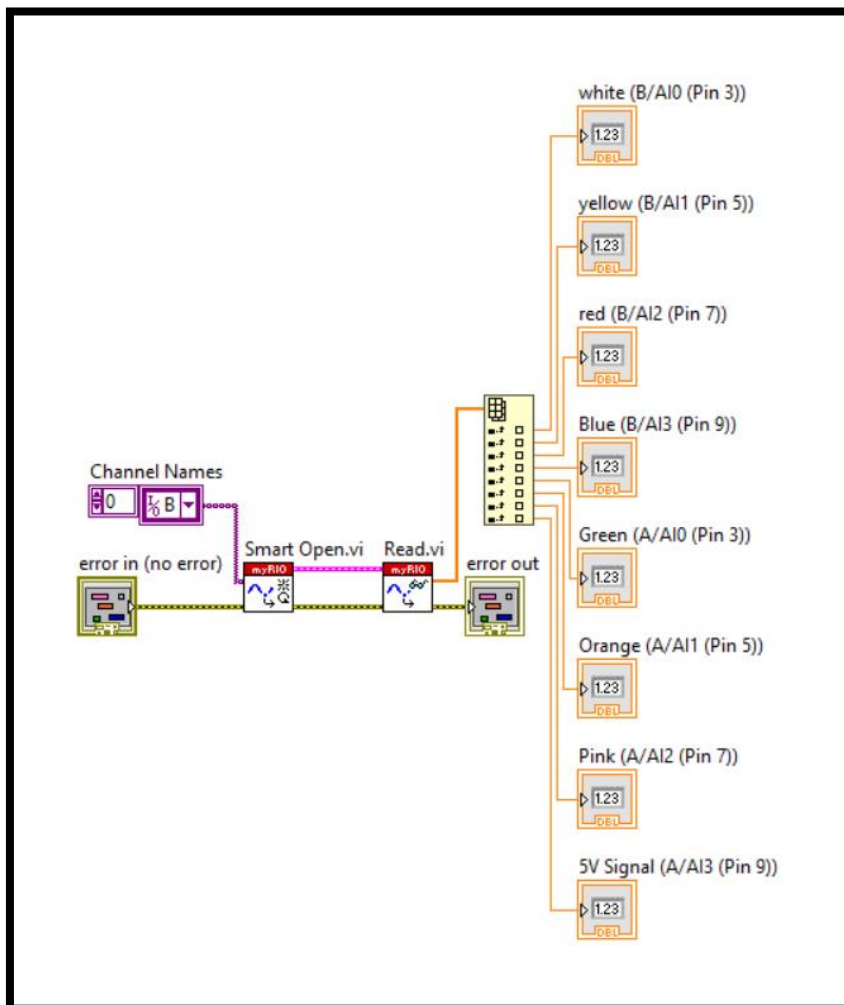


Figure 3.9 Analog input Express VI code

3.1.4.2. Digital Output Express VI

The Digital Output Express VI is shown in figure 3.10, it uses the MyRIO blocks mentioned in sections 3.1.2.1 and 3.1.2.2 to read a Boolean signal, which would activate the code inside the Digital Output Express VI code showed in figure 3.11 and send a 3.3 voltage out of the chosen pin.

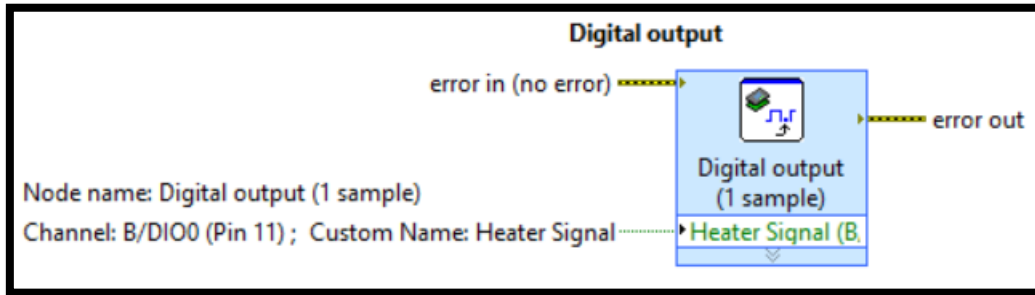


Figure 3.10 Digital Output Express VI

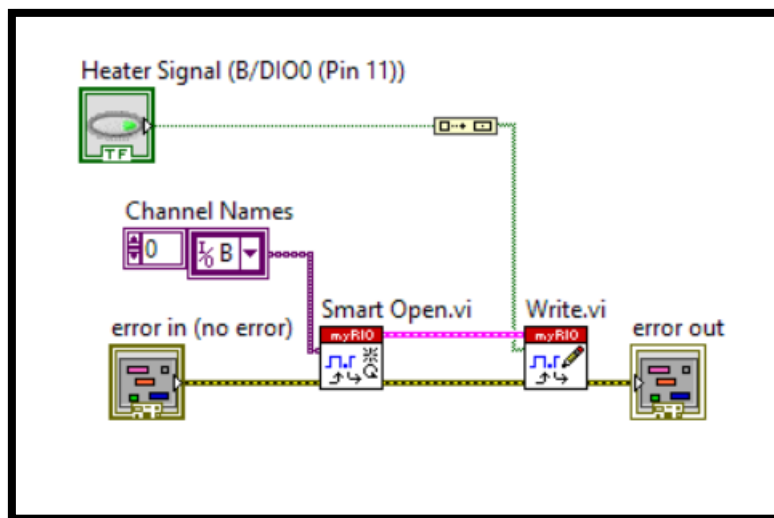


Figure 3.11 Digital Output Express VI code

3.2. Control Software for Laboratory experiments

During the complete process of developing the LabVIEW software, the software underwent many changes until the very end, when the team arrived at ZARM. The changes occurred for various reasons, such as having a better understanding of the airflow inside the test cell, deciding how to use the different drops provided by DYT or obtaining new knowledge about the LabVIEW blocks and SubVIs. Any actions that

impacted the experiment performance also affected the software design and vice versa.

The software design was developed to be able to function in different ways so that new changes would have a minimal impact on the software design. The idea was to develop the software design so that if a change occurred, the software design would have to make the minor changes possible.

The experiment software is divided into two VIs, a VI for the Matrix MXC-4000 and a VI for the MyRIO-1900. At this point, each VI contained the following parts:

MyRIO-1900 VI:

- Thermocouples code.
- Data acquisition code.
- Accelerometer code.
- Trigger codes.
- MyRIO-1900 Control Panel

As for the Matrix MXC-4000 VI:

- PZT code
- Microgravity time counter
- Matric MXC-4000 Control Panel

3.2.1. Experiment Flow Diagram

The idea of the experiment was to use the accelerometer inside the MyRIO to act as a trigger that would enable a microgravity counter, which would be used to active the devices. As shown in figure 3.12, the power supply to the heater, LED matrix, data acquisition and PZT, will be activated when a signal of 5V is received from the MyRIO.

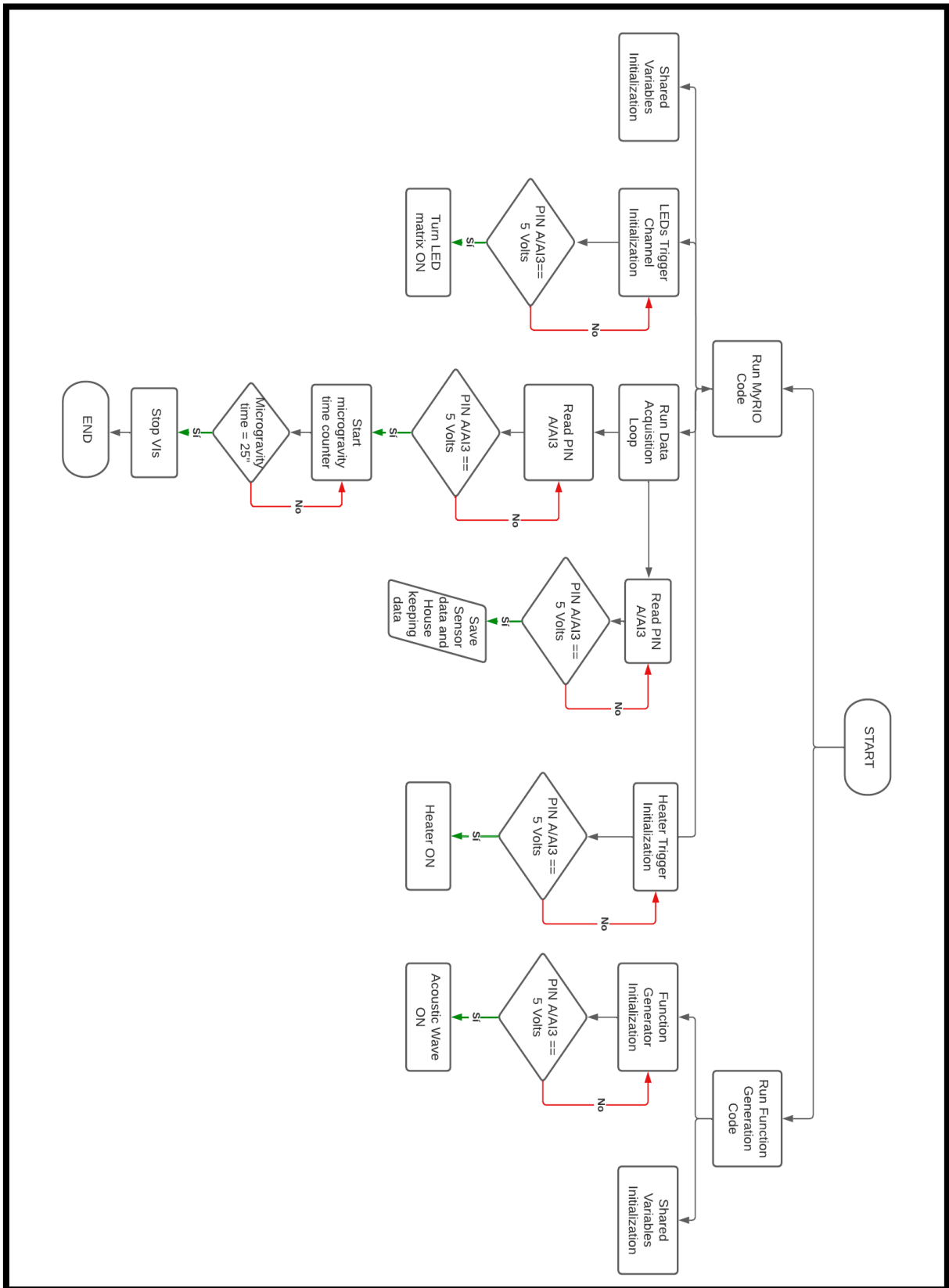


Figure 3.12 Experiment Flow Diagram

3.2.2. MyRIO-1900 VI

3.2.2.1. Thermocouples code

The thermocouples data is gathered by attaching the thermocouples to the analog input of connectors A and B from the MyRIO-1900. Then a calculation is done to change the voltage measured from the thermocouples to a temperature. The team member who designed the thermocouples circuit provided the necessary calculations and values.

To read the data from the thermocouples using LabVIEW, The Sub VI mentioned in section 3.1.4.1, was used. The Analog input Express VI reads data from 8 pins, four from connector A and four from connector B. 7 pins are used for the thermocouples while one is to read the 5V signal. The code of the thermocouples is shown in figure 3.13.

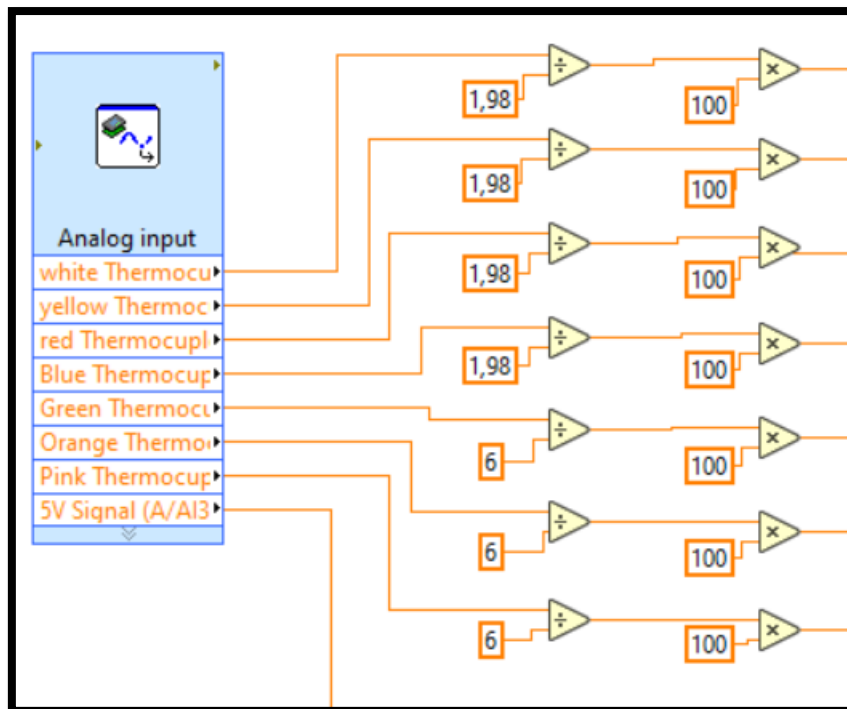


Figure 3.13 Thermocouples code

The pins selected in the Analog Input Express VI changed for the 5V signal as it was mentioned in section 3.1.4.1. At this point in time, the pins used for the thermocouples (and 5V signal) are shown in figure 3.14.

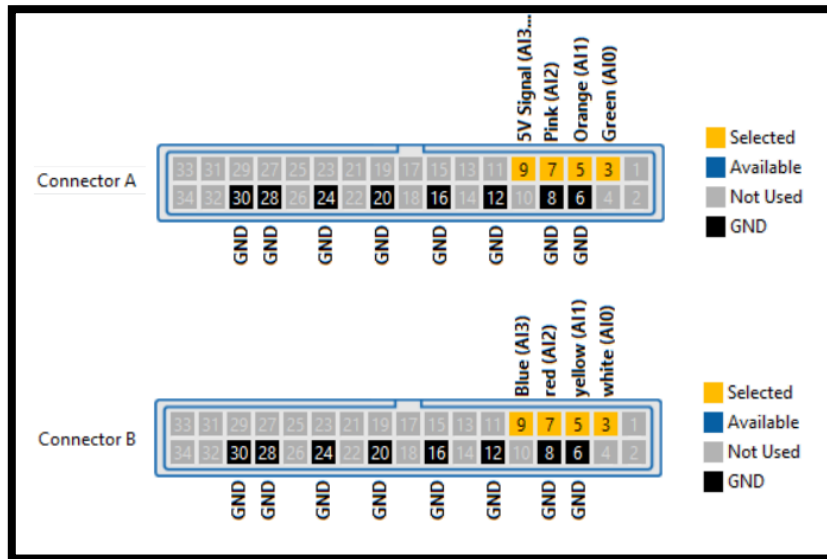


Figure 3.14 MyRIO pins in use

3.2.2.2. Data acquisition code

The data acquisition code contains two parts. The first part, shown in figure 3.15, uses the Open/Create/Replace file block to open or create a file. The name, where it should be created, and the file type is also stipulated here. The document created in the MyRIO-1900 memory for this experiment is a .txt file.

Then the information from the Open/Create/Replace file block is given to the Write Delimited Spreadsheet VI, which will create the headings of each column. In order to separate the headings, all the heading's names are added to a matrix and separated each name with a 'coma' in the matrix.

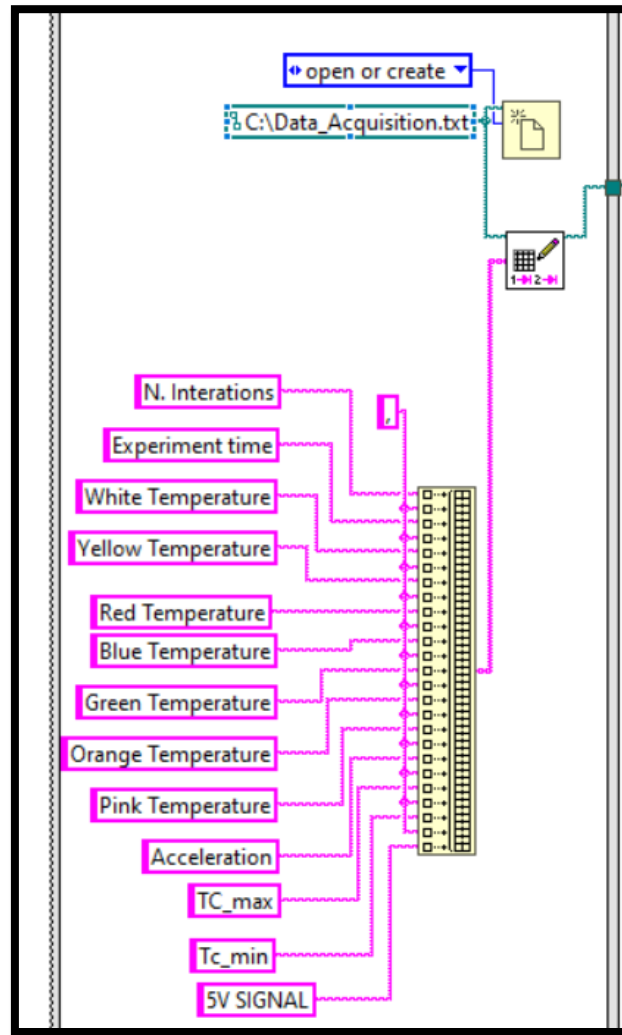


Figure 3.15 Data acquisition initialization [18]

Once the file with the headings is created, the new file path is sent to another Write Delimited Spreadsheet VI (shown in figure 3.16), which collects the data to be gathered for data acquisition and housekeeping, as mentioned before, a 'coma' is used to separate the data.

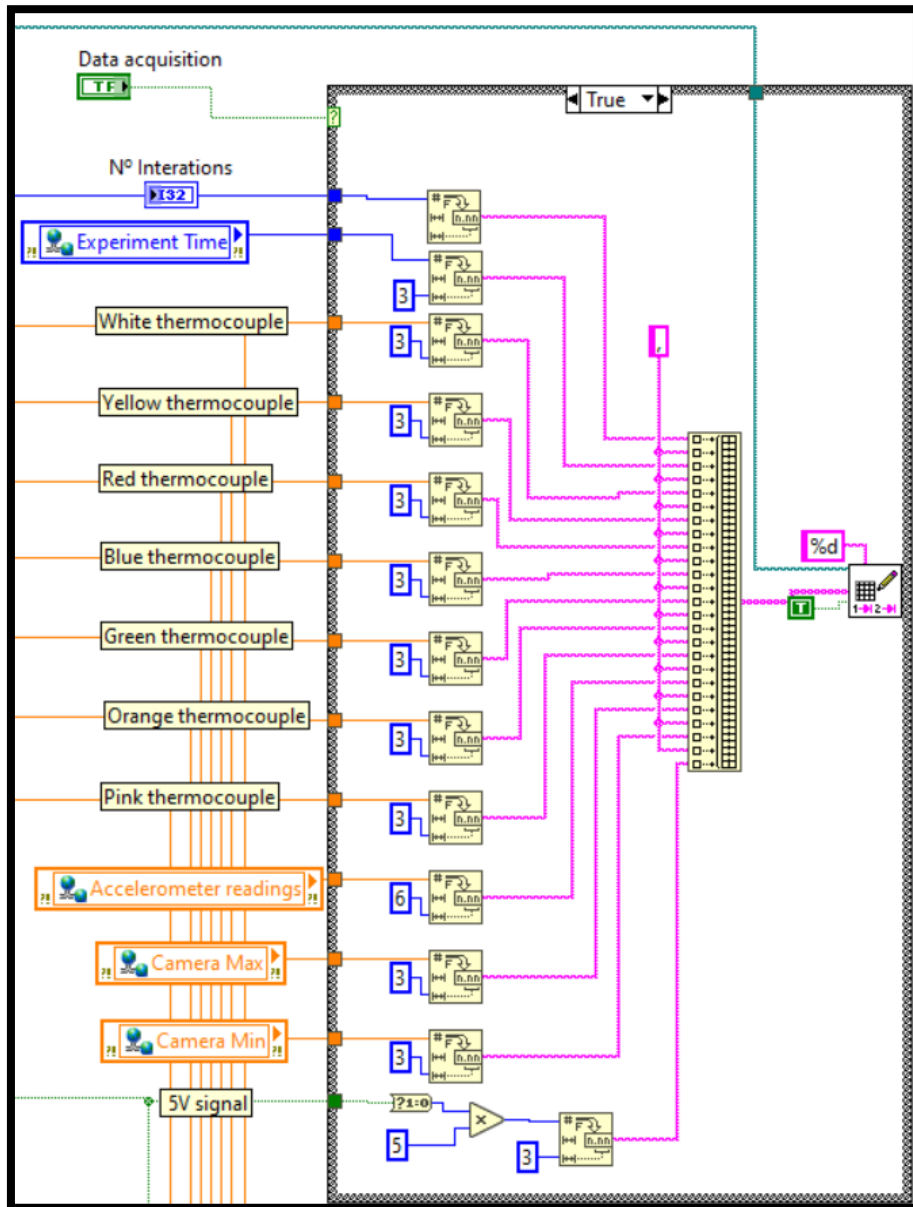


Figure 3.16 Data acquisition and housekeeping [18]

3.2.2.3. Accelerometer Code

The acceleration that the experiment is experiencing is determined by the accelerometer that the MyRIO-1900 contains. A SubVI obtained from the MyRIO palette is used to show the accelerometer's readings using LabVIEW. This SubVI reads the acceleration in the three axes, as shown in figure 3.17. The net acceleration is obtained using simple mathematic calculations.

A microgravity trigger will be enabled if the acceleration is lower than 0,2 [m/s²] and the 5V signal from the PXI is obtained.

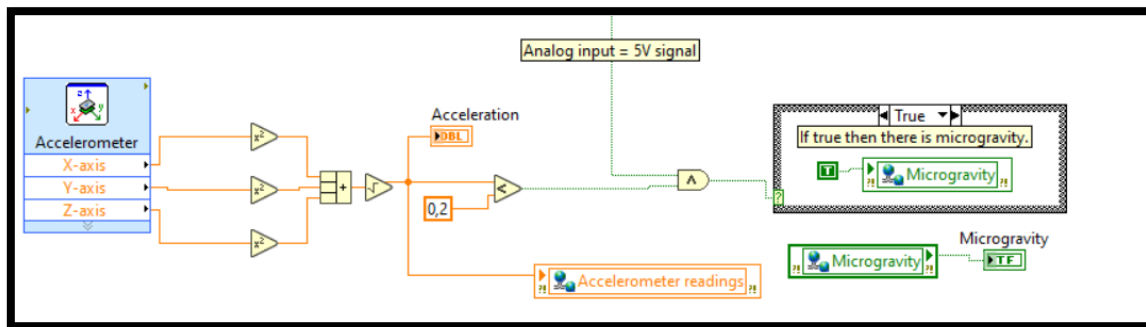


Figure 3.17 Accelerometer code

3.2.2.4. Triggers Code

There are three different types of triggers. The first one is to activate the heater, which consists of four cases, each depending on the temperature that was wanted for the heater to reach. The second type of trigger was meant for the LED matrix. Both types of triggers depended on the virtual microgravity trigger, as shown in the previous section. The last type of trigger was developed in case it was necessary to initiate some device based on the experiment timer.

Figure 3.18 shows the heater and LED matrix triggers. It uses the MyRIO main blocks explained in section 3.1.2. On the left side of figure 3.18 are the four heater channels and the LEDs channel. Only one heater trigger can be activated at a time. This is done by using a case structure. The case structure has five different cases. Each case allows the heater to reach different temperatures 0 (default), 50, 70, 100, and 140 degrees Celsius. However, the triggers can only be activated if the case structure is set as TRUE and the microgravity trigger has been enabled. The LED matrix trigger is turned on as soon as the microgravity trigger is enabled.

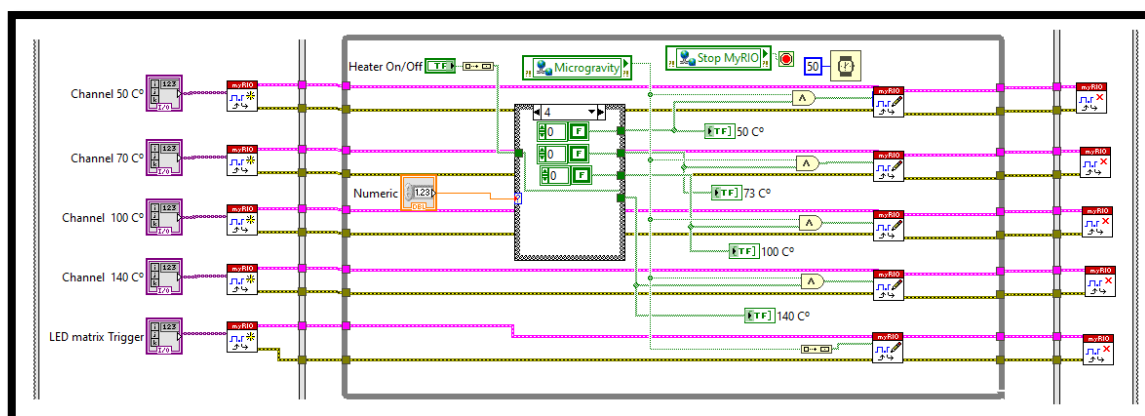


Figure 3.18 Heater trigger and LED trigger

The time trigger shown in figure 3.19, uses the shared variable “experiment time” to activate the trigger, this occurs when the experiment time is equal or greater than the stated value in the code, in this example the stated value is 5 seconds.

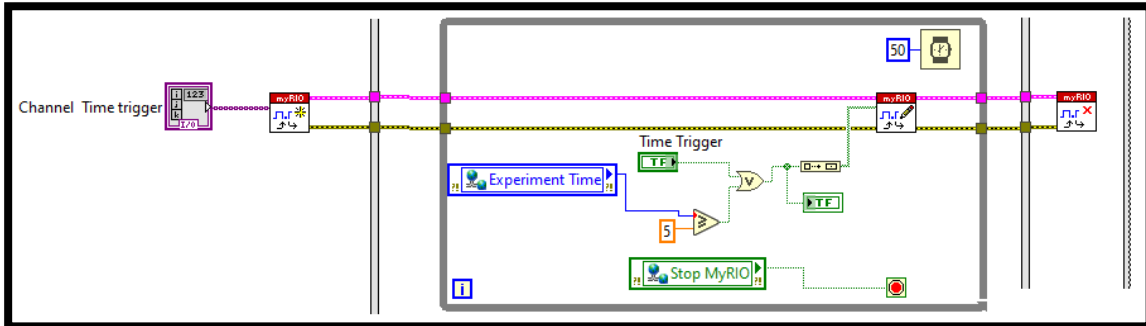


Figure 3.19 Time Trigger

The experiment time, shared variable, is obtained from the experiment timer code, shown in figure 3.20. The experiment time is obtained by using the Tick Count block that has the functionality of counting, by subtracting the value from inside the while loop, which is constantly running, with the value from outside the while loop, the experiment time is obtained, then it is divided by 1000, as the Tick Count block counts in milliseconds.

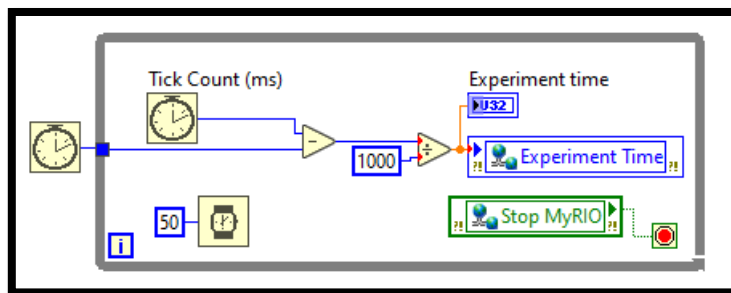


Figure 3.20 Experiment timer

All the described triggers used the low level block, which are shown in section 3.1.2. The triggers need a path which is selected from the control panel, figure 3.21 shows the triggers paths (pins).

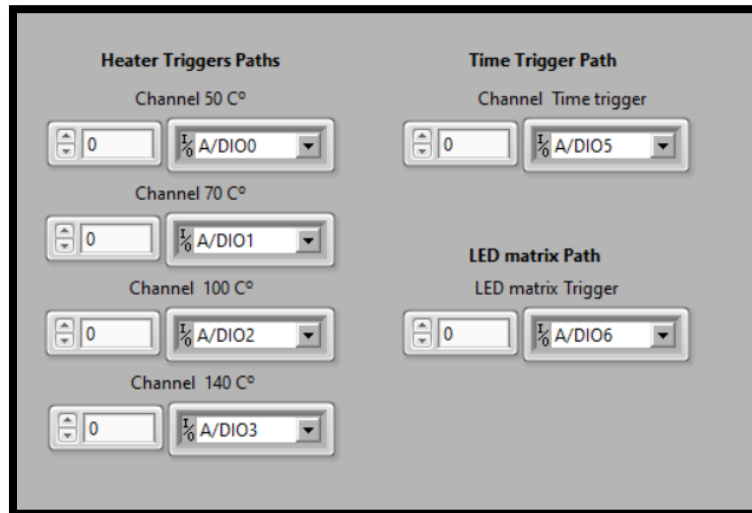


Figure 3.21 Triggers Paths

3.2.2.5. Control Panel

The MyRIO-1900 control panel, shown in figure 3.22, represents the majority of the information that the experiment provided at this point, except for the information of the PZT frequencies and amplitude.

The control panel is composed of the main panel on the left side and the wave chart on the right. The wave chart shows the thermocouple's readings. The panel is used to control the experiment.

At the top part of the panel is the heater trigger. From left to right, it shows the push button to activate it, the numeric control to choose the heater configuration, and the maximum temperature the heater can reach, shown with four different LEDs.

Under the 4 LEDs, there is the Push button to activate the time trigger, a LED to indicate that the time trigger is activated, a data acquisition button, and a LED to indicate the status of the Microgravity.

Then there is a numeric controller to choose the temperature threshold for the heater and a LED to indicate if the heater reached this temperature. A Stop button which stops the MyRIO-1900 VI and the Matrix MXC-4000 VI, is used in case of an emergency.

Next to the Stop button, ten numeric indicators give the readings of the seven thermocouples, the number of interactions of the data acquisition loop, the experiment time in seconds and the acceleration.

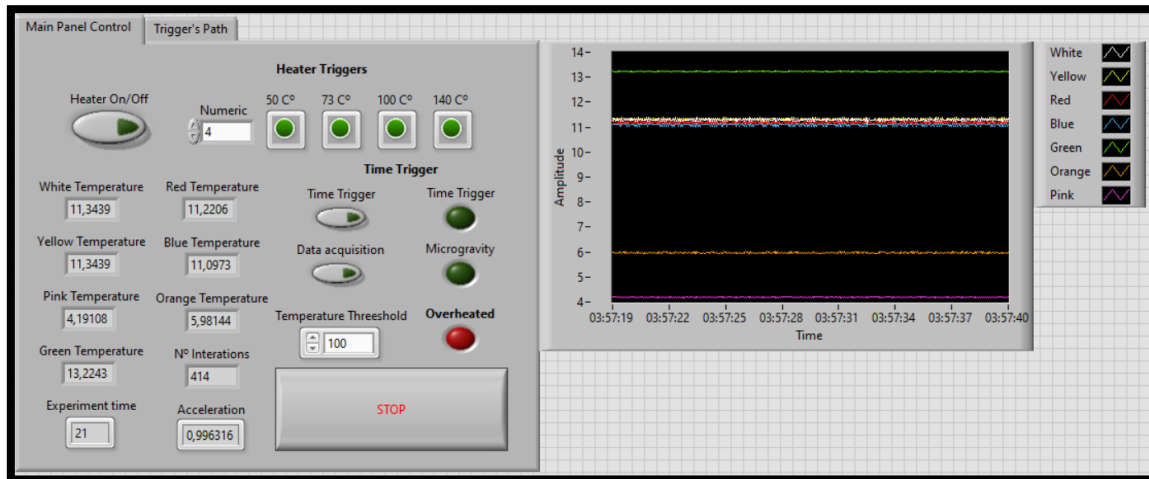


Figure 3.22 MyRIO-1900 Control Panel

3.2.3. Matrix MXC-4000 VI

As it was mentioned in section 3.1.3, the Matrix MXC-4000 is used to active the PZT at the desired frequency and amplitude, at this point in time, there was an idea of changing the frequency in the middle of the drop. Therefore, the function generator code also contains a microgravity time counter code, it uses the same principal as the experiment timer code.

3.2.3.1. PZT code

Figure 3.23 shows the function generator code with the microgravity timer at the top. The first step was to develop the experiment timer code, but in this case, instead of using two tick counters, only one and a shift register were used. By using the shared variable "microgravity trigger", connected to a case structure with a tick counter inside, to measure the time until the microgravity trigger is activated, then this value is subtracted from the experiment time.

The main blocks of the PZT code are the Matrix MXC-4000 blocks described in section 3.1.3. The PZT has three ways to be activated. The first one is by a Boolean push button. The second way is by using the microgravity trigger, but as in the first and third ways, the push button must be activated. Lastly, the third way to activate it is by using a stated microgravity time. In the case of the showed code, the time was stated to be 0,1 seconds.

Once the PZT is activated, it will emit the "frequency 1" (kHz), frequency 2 (kHz) and amplitude (V) chosen by numeric control. The times at which each frequency starts and ends are selected with contacts. Frequency 1 would start when the microgravity timer reaches 1 second and end when it reaches 15 seconds. Frequency 2 starts at

the second 15 and ends at the second 60. However, these times were only used for testing.

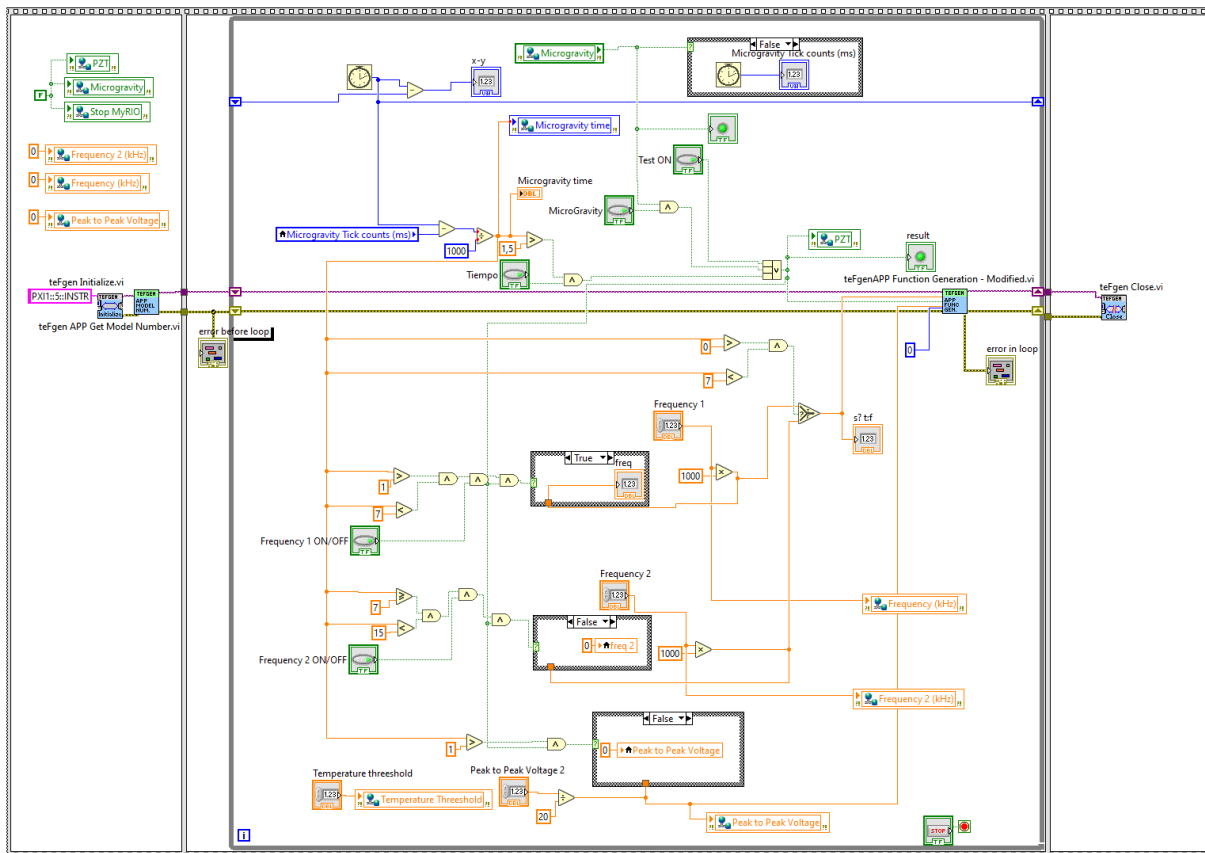


Figure 3.23 PZT code [18]

3.2.3.2. Control Panel

The Matrix MXC-4000 control panel presented in figure 3.24, shows the push buttons to activate the PZT and the frequencies, virtual LEDs to inform when microgravity and the PZT are ON. Numerical indicators are used to indicate the peak to peak voltage output, the microgravity time and the frequencies. Numerical controls are used to state the peak to peak voltage, frequency 1 and frequency 2.

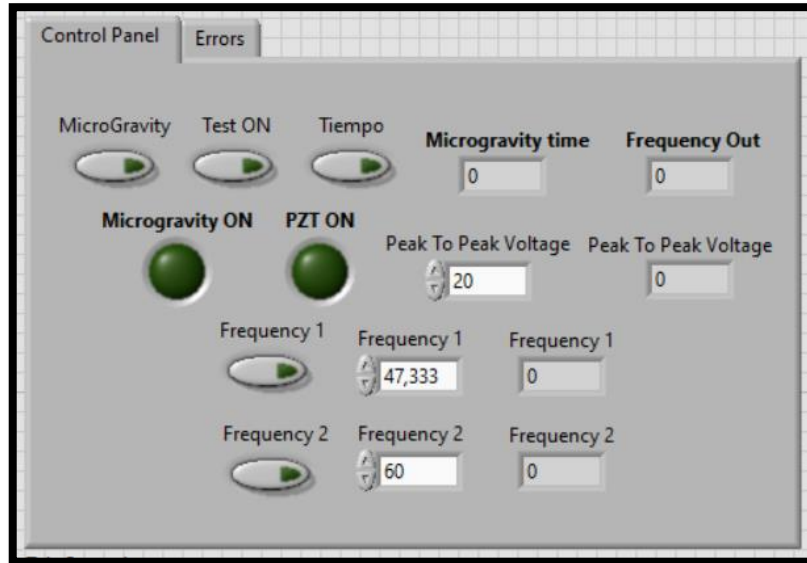


Figure 3.24 Matrix MXC-4000 control panel

3.3. Control software for Drop Tower Experiments

The software was simplified and adjusted until the end of the assembly week in ZARM, when it was finally completed. The software was possible to be simplified, due to the following reasons:

The first one was thanks to the knowledge obtained from the mathematical simulation, which provided the final experiment performances, giving the software the capability to focus on a specific design.

The second reason was the use of the windows remote control application, which is not directly mentioned in the ZARM user manual [17], but it is mentioned that the capsule is equipped with a radio telemetry / telecommand system, this system provides an industrial, wireless local area network transmission path. As a result of a lack of knowledge in this area, the idea for the communication was to develop a RS-232 protocol, the RS-232 protocol code, was never finished as it was proved to be unnecessary.

3.3.1. Experimental Procedure

The following table (table 3.1) shows the steps that had to be taken before and after each drop. The windows remote control application, allowed the team to control the Matrix MXC-4000 and work as if the experiment was being done in the laboratory.

Table 3.1 Experimental Procedure

Time	Action	Description
T -180"	PZT configuration	The PZT is configured to be activated or not during the experiment, the frequency to be tested is checked.
T -120"	Data acquisition ON	The data acquisition is activated.
T = -1"	PZT power supplied	The PZT is powered, if in the configuration it is turned on, an acoustic wave would be created.
T = 0	Microgravity	The capsule accelerometer reaches microgravity.
T = +0,5"	Heater ON	After the shock from the launch, the heater is activated.
T = +15"	Data acquisition Download	After the capsule has landed the data acquisition is downloaded.

3.3.2. MyRIO-1900 VI

In this section the last form of the MyRIO-1900 LabVIEW codes will be shown. it will have a similar structure than section 3.2.2, but with the absent of the data acquisition and the microgravity time counter as these codes had almost no changes. The biggest change is the fact that the accelerometer code is not used anymore, because the 5V signal from the capsule PXI is used as the microgravity virtual trigger, some changes are shown in the thermocouples code, heater trigger code and the control panel.

3.3.2.1. Thermocouples code.

In comparison with the Thermocouples code in section 3.2.2.1, the name of the thermocouples has been changed as well as the calculations that have to be done to the thermocouples, due to changes in the sensor circuit. Also the “5V signal” has been changed for “heater signal”. The Analog input Express VI now uses 7 pins from connectors A and B instead of the 8 pins from before, as it uses connector C for the heater signal. This was done because connector C has 2 analog inputs that withstand voltages from -10 to +10, making it the most reliable analog input.

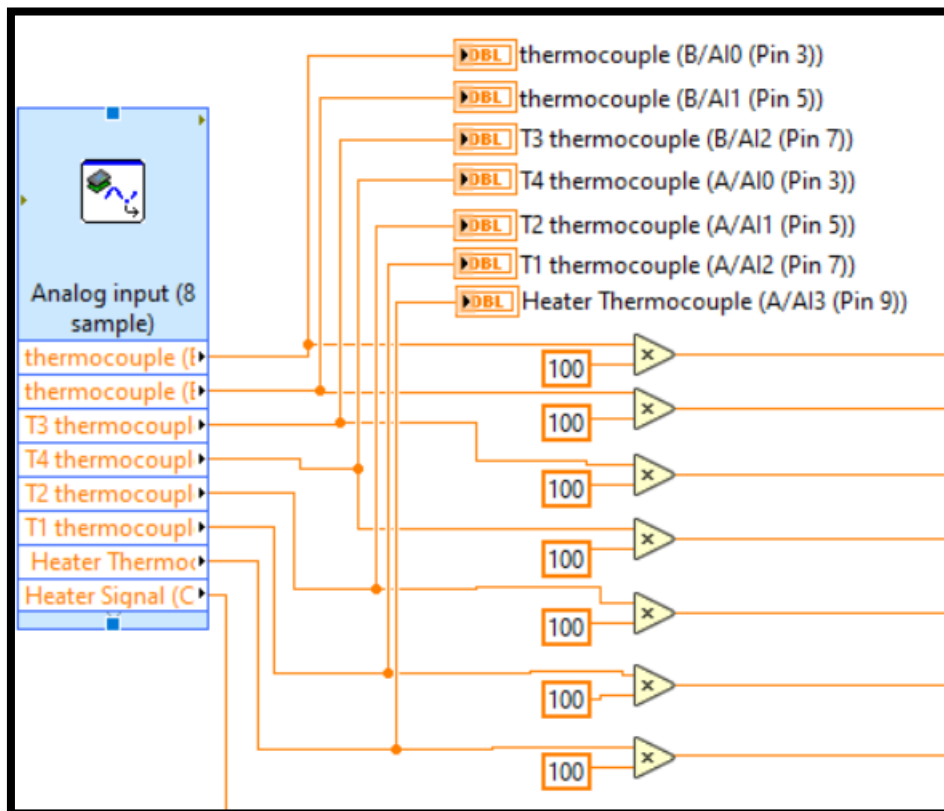


Figure 3.25 Updated Thermocouples code

3.3.2.2. Heater Trigger Code

The heater trigger code uses the Digital Output Express VI described in section 3.1.4.2, to activate the heater power supply trigger. It also starts the microgravity counter.

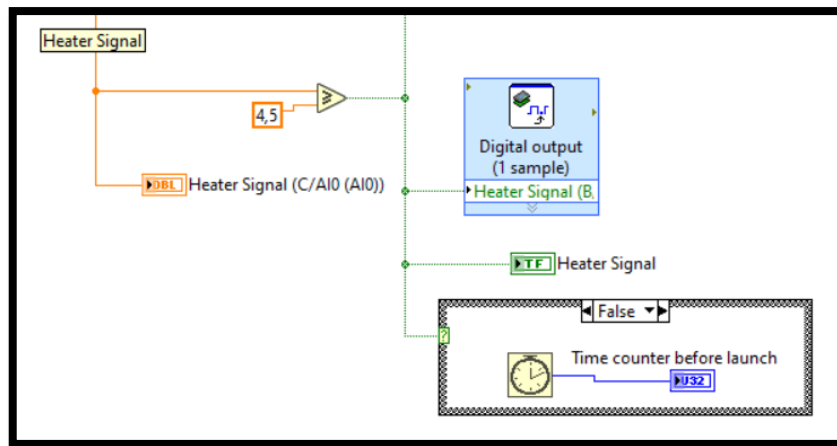


Figure 3.26 Updated Heater Trigger code

3.3.2.3. Control Panel

Figure 3.27, shows the MyRIO-1900 VI control panel, the control panel consists of a wave chart, to see the changes in temperature. The thermocouple readings are shown as indicators, in the form of a voltage and temperature. There are two virtual LEDs, both at the bottom left of the control panel, under the data acquisition push button, the LED at the left is to inform that the MyRIO-1900 is collecting the data, and the one next to it to show when the heater is ON. At the right side of the heater LED, there are three indicators, to show the experiment time, microgravity time and the voltage obtained from the PXI. The control panel also shows a push button in red to stop the MyRIO-1900 VI as well as the Matrix MXC-4000 VI.

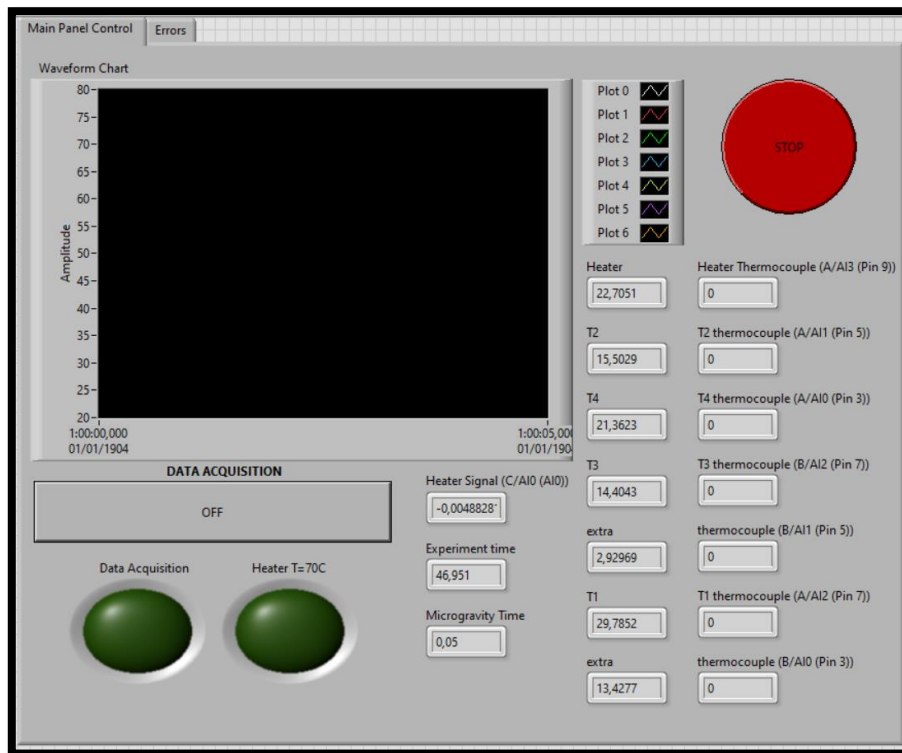


Figure 3.27 Updated MyRIO-1900 VI control panel

3.3.3. Matrix MXC-4000 VI

3.3.3.1. PZT code

The PZT code was simplified, as the idea of activating a different frequency in the middle of the drop wasn't appropriate, due to the results being difficult to be processed.

Therefore, the final code just shows the Matrix MXC-4000 blocks, a push button to activated the PZT at the desired time, and two numeric controllers to specify the frequency and amplitude.

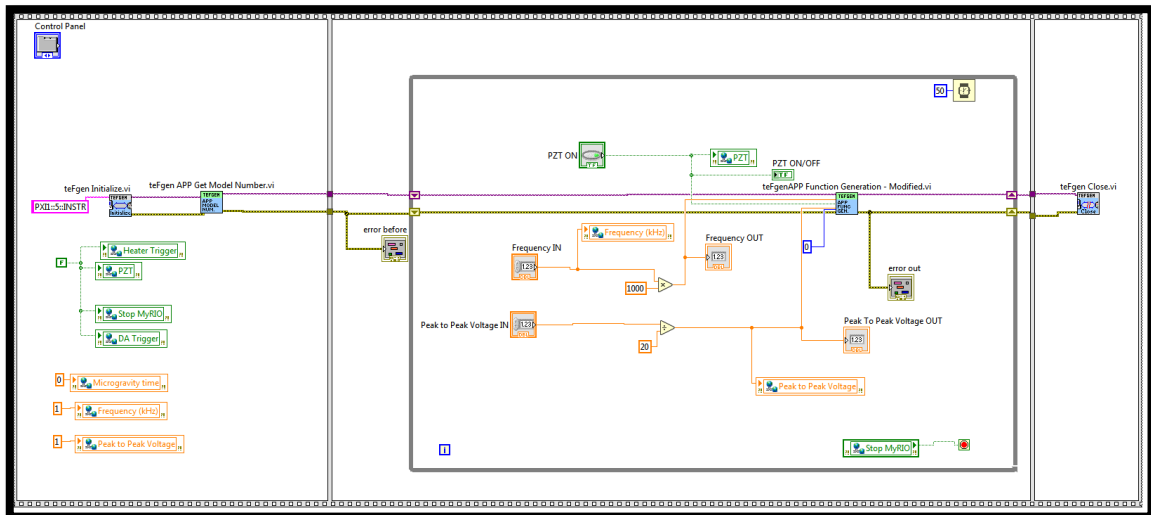


Figure 3.28 Updated PZT code

3.3.3.2. Control Panel

The control panel is a representation of the code in the VI, as the PZT code was simplified, the same occurred to the control panel. In this control panel only the Frequency and the Peak to peak voltage (amplitude) are maintained from the controllers, the rest are indicators, and a push button to active the PZT, as well as a virtual LED to indicate that it is ON. The rest are indicators of the frequency output, peak to peak voltage and the Matrix MXC-4000 VI running time.

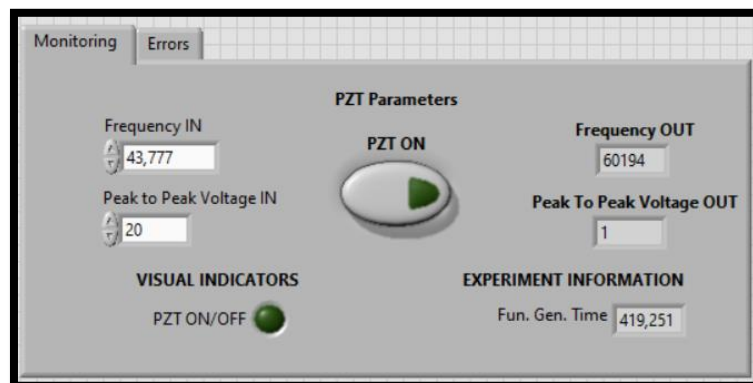


Figure 3.29 Updated Matrix MXC-4000 VI control panel

Chapter 4

CONCLUSION

The master's thesis experiment presented in this thesis continues a previous experiment [3] done at the Space Exploration Lab at the Universitat Politècnica de Catalunya. The previous experiment [3] showed an increase in heat flux of more than 8% on earth and under microgravity conditions. Initiating the idea of using acoustic waves for heat transfer enhancement but in a gas medium. After some research, it was shown that even though other experiments had used acoustic waves for heat transfer enhancement in a gas medium, as mentioned in section 1.2, it would be the first time applying it under microgravity conditions.

Therefore, a new team of 5 master students was created under professor Ricard Gonzalez Cinca. The students and professor applied for the drop your thesis programme. To have the possibility to carry out the experiment under microgravity conditions.

The experiment was divided into five fields having one master student taking control of it. The fields were mathematical simulations, testing, electrical design, mechanical design and software design. This master's thesis is based on the software design of the experiment, using the LabVIEW platform to control the experiment on earth, at the Space Exploration Lab and under microgravity conditions, at the ZARM Drop Tower.

The experiment control was developed based on the needs that the other members of the team had. However, as the experiment procedure at the Drop Tower was unclear, the control software had to be designed to consider any possible variable. For example, developing many different types of triggers or having the possibility of changing the acoustic wave frequency during the experiment.

As a result, the control software of the experiment was a success, and it was even possible to be simplified during the integration week at the ZARM drop tower. The control software development could have been done faster and more straightforwardly from the beginning. However, a longer path was taken due to the need for more knowledge and experience in this field.

To conclude, the experiment software design had many ups and downs during the time it took to familiarise myself with the LabVIEW platform and design the experiment software. Nevertheless, the result is a successful LabVIEW code that controls a heater and a PZT, gathers data from thermocouples and saves it in a .txt file inside of the MyRIO-1900, which can be accessed at any moment.

Chapter 5

BIBLIOGRAPHY

5.1. Articles:

[1] Laetitia Mottet. Heat and mass transfer in the porous wick of a capillary evaporator. 06/2014.

[2] Karthekeyan Sridhar, Ryan Smith, Vinod Narayanan, and Sushil Bhavnani. Phase change cooling of spacecraft electronics: Terrestrial reference experiments prior to ISS microgravity experiments. In 2020 19th IEEE Intersociety Conference on Thermal and Thermomechanical Phenomena in Electronic Systems (ITherm), pages 315–322, July 2020.

[3] Guillem Quintana-Buil and Ricard González-Cinca. Acoustic effects on heat transfer on the ground and in microgravity conditions. *International Journal of Heat and Mass Transfer*, 178:121627, 2021.

[4] Alessandro Franco and Carlo Bartoli. Heat Transfer Enhancement due to Acoustic Fields: A Methodological Analysis. *Acoustics*, 1(1):281–294, 2019.

[5] Mathieu Legay, Nicolas Gondrexon, Stéphane Le Person, Primius Boldo, and André Bontemps. Enhancement of heat transfer by ultrasound: Review and recent advances. *International Journal of Chemical Engineering*, 2011, 2011

[6] M. K. Aktas, B. Farouk, and Y. Lin, “Heat transfer enhancement by acoustic streaming in an enclosure,” *J. Heat Transfer*, vol. 127, no. 12, pp. 1313–1321, 2005, doi: 10.1115/1.2098858.

[7] S. J. Lighthill, “Acoustic streaming,” *J. Sound Vib.*, vol. 61, no. 3, pp. 391–418, Dec. 1978, doi: 10.1016/0022-460X(78)90388-7.

[8] B. G. Loh and D. R. Lee, “Heat transfer characteristics of acoustic streaming by longitudinal ultrasonic vibration,” *J. Thermophys. Heat Transf.*, vol. 18, no. 1, pp. 94–99, 2004, doi: 10.2514/1.9156.

[9] L. Slimani, A. Bousri, A. Hamadouche, and H. Ben Hamed, “Numerical and Experimental Study of Heat Transfer Enhancement with Metal Foams and Ultrasounds,” vol. 15, no. 5, pp. 202–207, 2021.

[10] M. Talebi, M. Setareh, M. Saffar-Avval, and R. Hosseini Abardeh, “Numerical investigation of natural convection heat transfer in a cylindrical enclosure due to ultrasonic vibrations,” *Ultrasonic*, vol. 76, pp. 52–62, 2017, doi: 10.1016/j.ultras.2016.12.010.

5.2. Web Pages

[11] European Space Agency. (n.d.). *ESA education*. Retrieved January 20, 2023, from <https://www.esa.int/Education>

[12] ESA. *Rexus*. Rexus/Bexus. Retrieved December 9, 2022, from <http://reusbexus.net/rexus/>

[15] National Instruments. *¿Qué es LabView? Programación Gráfica Para Pruebas y medidas*. NI. Retrieved December 5, 2022, from <https://www.ni.com/es-es/shop/labview.html>

[16] National Instruments. *Sistemas Pxi*, NI. Retrieved December 5, 2022, from <https://www.ni.com/es-es/shop/pxi.html>

5.3. Datasheets:

[13] National Instruments. (June, 2018). *User Guide and Specifications NI MyRIO.1900*. Retrieved December 9, 2022, from <https://www.ni.com/docs/en-US/bundle/myrio-1900-getting-started/resource/376047d.pdf>

[14] ADLINK Technology. (January 24, 2014). *Matrix MXC-4000 Series* from https://www.adlinktech.com/Products/Download.ashx?type=MDownload&isDatasheet=yes&file=1039%5CMXC-4000Series_Datasheet_en_1.pdf

[17] ZARM. (March 01, 2022). *Bremen Drop Tower Payload user's guide*. Version 1.1 pages 19-20

5.4. Thesis

[18] Sergi, A., & Soler, B. (n.d.). *Títol: Design and integration of the electronic parts of a suborbital payload*.